Dynamic Response Analysis of Spar Buoy Floating Wind Turbine Systems

by

Sungho Lee

B.S. Mechanical Engineering
Illinois Institute of Technology, 2005

SUBMITTED TO THE DEPARTMENT OF MECHANICAL ENGINEERING IN PARTIAL FULLFILLMENT OF THE REQUIREMENTS FOR THE DEGREE OF

MASTER OF SCIENCE IN MECHANICAL ENGINEERING

AT THE

MASSACHUSETTS INSTITUTE OF TECHNOLOGY

JUNE 2008

Author:.....
Sungho Lee
Department of Mechanical Engineering
May 18,2008

Certified by:.....
Paul D. Sclavounos
Professor of Mechanical Engineering
Thesis Supervisor

Accepted by:.....
Lallit Anand
Professor of Mechanical Engineering
Chairman, Committee on Graduate Students

Dynamic Response Analysis of Spar Buoy Floating Wind Turbine Systems

by

Sungho Lee

Submitted to the department of Mechanical Engineering
on May 19, 2008 in partial fulfillment of the
requirements for the degree of
Master of Science in Mechanical Engineering

Abstract

The importance of alternative energy development has been dramatically increased by the dwindling supplies of oil and gas, and our growing efforts to protect our environment. A variety of meaningful steps have been taken in order to come up with cleaner, healthier and more affordable energy alternatives. Wind energy is one of the most reliable energy alternatives for countries that have sufficiently large wind sources. Due to the presence of steady and strong winds, and the distance from coastline residential, the offshore wind farm has become highly attractive as an ideal energy crisis solution.

Floating wind turbine systems are being considered as a key solution to make the offshore wind farm feasible from an economic viewpoint, and viable as an energy resource. This paper presents the design of a synthetic mooring system for spar buoy floating wind turbines functioning in shallow water depths. Nacelle acceleration, static and dynamic tensions on catenaries, the maximum tension acting on the anchors are considered as design performances, and a stochastic analysis method has been used to evaluate those quantities based on sea state spectral density functions. The performance at a 100-year hurricane condition is being defined as a limiting case, and a linear wave theory has been the most fundamental theory applied for the present analysis.

Thesis Supervisor: Paul D. Sclavounos
Title: Professor of Mechanical Engineering

Acknowledgements

I would like to sincerely express my gratitude to Professor Paul D. Sclavounos for his thoughtful guidance and inspiration in my research during the past two years in MIT. I couldn't accomplish this research result without his continuous inspiration and profound knowledge about offshore wind energy technology which is now contributing not only to MIT energy initiative, but also to world alternative energy resource development. I'm sincerely grateful to him for providing me with all these opportunities, and for his endless patience.

I also would like to thank the LSPF alumnus, Christopher Tracy and Elizabeth Wayman for their initial contribution to develop the hydrodynamic analysis codes for analysis of floating wind turbine, and my current colleagues in the LSPF, Kyriakos Avgouleas, and Joshua Di Pietro for their great support. I also would like to specially thank Hyunjoe Kim for his helpful advice on my work and his endless willingness to answer any question.

Finally I would like to thank to my families and especially Jieun Choi for her endless patience and indescribable support. I couldn't complete this work without her.

Contents

1. Introduction and background

To date almost all large scale offshore floating structures were designed and built to meet the needs of the offshore oil and gas industry. A variety of these hydrocarbon platforms are located off of the continental shelf in water depths of up to a few kilometers. The current designs for floating platforms and mooring systems have been focused on optimization of dynamic performance in these extreme water depths.

Meanwhile, the optimal locations for an offshore wind farm with the best wind resource, the least cost, and the least visibility from onshore are most likely located in an intermediate-shallow water depth of approximately 50 ~ 300 meters. An offshore wind turbine with a foundation of fixed monopiles can not be technically or economically feasible in these water depths. A promising solution can be offered by an innovative idea, a wind turbine system based on the floating platform technology. However, the dynamic motion behavior of floating wind turbines at this shallow water is essentially different from the ones in deep water. The mooring line design is an especially challenging problem in the design of these intermediate depth floating structures.

The majority of conventional mooring systems of offshore floating structures have been based on a steel catenary mooring line in which the restoring force for station keeping is developed by the weight of the steel mooring line. In shallow water, the unit weight of the steel has to be dramatically increased in order to provide a sufficient restoring force with a reasonable foot print in such a shallow water depth. The weight of the steel mooring lines, at the same time, has to be supported by the buoyancy of the platform, which will be inevitably huge in this case. This becomes a serious design problem. A synthetic fiber mooring system has a much lighter weight, and also provides a strong restoring effect which can shift the motion RAO peaks away from the sea spectrum band. This is why a synthetic fiber mooring system is being considered as a promising alternative system against a steel mooring line in shallow water.

2. Design Base Lines

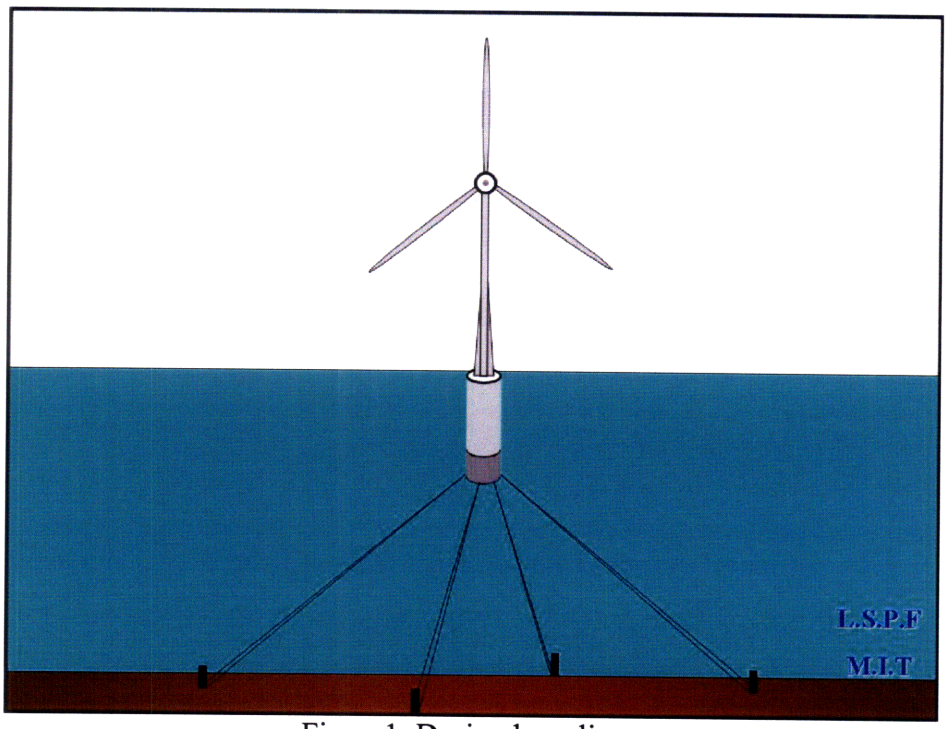

Figure1. Design base lines

A spar buoy has been selected as a base platform. It is modeled as a rigid symmetrical cylinder with catenary mooring lines attached at the bottom of the cylinder in four separate quadrants. This provides the stability and stiffness on the entire system. It is assumed that the platform is being connected to the seabed by four mooring anchors separated from each other by 90 degree as shown on the 3-dimensional figure above. The vertical location of fairlead, of course, is one of the design parameters, which will be taken account for the Pareto simulation analysis.

The initial pretension is assumed to be equal for all catenary mooring lines in a given layer. However, a quasi-static equilibrium position of the entire system due to wind thrust is determined by iteration analysis, and the effective initial pretension at this position becomes non-uniform along the lines. The corresponding forces from catenary mooring lines at the initial or quasi-static equilibrium position, and the wave exciting forces including the diffraction effects at the initial position are evaluated by

LINES and WAMIT respectively under a finite water depth condition. The seabed and the free surface is assumed to be completely parallel to each other.

A viscous damping force including VIV (Vortex Induced Vibration) and any possible current velocity acting on the platform and mooring lines are not considered. A viscous force possibly acting on the platform by vertical damping plates will be studied separately at the end of chapter 5.

2.1. The Wind Turbine

The basis wind turbine that has been used for the present system is the NREL baseline 5 MW wind turbine, and its specification has been tabulated below.

Properties		As-designed	Units
Hub height		90	m
Hub diameter		3	m
Rotor diameter		126	m
Total mass		700	metric tons
Center of gravity	X	-0.2	m
	Y	0	m
	Z	64	m
Wind speed		11	m/s
Turbine thrust		80	metric tons
Turbine moment		7200	metric tons-m
Maximum tip speed		80	m/s
Maximum rotor speed		12.1	rpm

Table1. The NREL baseline 5MW wind turbine specifications

During operation, this NREL wind turbine is capable of generating a maximum thrust load of 80 metric tons, and therefore generating a total torque of 7.2E07 Nm about the free surface.

The mass, damping, and restoring matrix for the above NREL 5MW wind turbine has been evaluated by FAST as shown below.

$$M_{WT} = \begin{bmatrix} 0.7 & 0 & 0 & 0 & 44.3 & 0 \\ 0 & 0.7 & 0 & -44.3 & 0 & 6.6 \\ 0 & 0 & 0.7 & 0 & -6.6 & 0 \\ 0 & -44.3 & 0 & 3499 & 0 & 0 \\ 44.3 & 0 & -6.6 & 0 & 3560 & 0 \\ 0 & 6.6 & 0 & -513.3 & 0 & 101.2 \end{bmatrix} \times 10^6$$

$$B_{WT} = \begin{bmatrix} 0.04 & 0 & -0.01 & -0.25 & 4.00 & 0.08 \\ 0 & 0 & 0 & -0.11 & -0.18 & -0.05 \\ -0.01 & 0 & 0 & -0.04 & -0.92 & -0.33 \\ 0.27 & -0.10 & 0 & 16.17 & 50.30 & 13.88 \\ 3.42 & 0.06 & -1.00 & -23.92 & 400.10 & 59.01 \\ 0.05 & -0.02 & 0.22 & 11.08 & -52.60 & 101.2 \end{bmatrix} \times 10^6$$

$$C_{WT} = \begin{bmatrix} 0 & 0 & 0 & 0.3 & 0.2 & 0 \\ 0 & 0 & 0 & -0.1 & 0.3 & -0.07 \\ 0 & 0 & 0 & -0.3 & -0.4 & 0 \\ 0 & 0 & 0 & 8.5 & -22.4 & 59.7 \\ 0 & 0 & 0 & 26.8 & 28.9 & -4.1 \\ 0 & 0 & 0 & -1.2 & 1.1 & -4.8 \end{bmatrix} \times 10^6$$

Mass, damping, and stiffness matrix of NREL 5 MW wind turbine

2.2. The Platform

The hydrodynamic properties of a spar platform of 14 m in diameter and 60 m in draft has been evaluated by WAMIT and plotted as shown below.

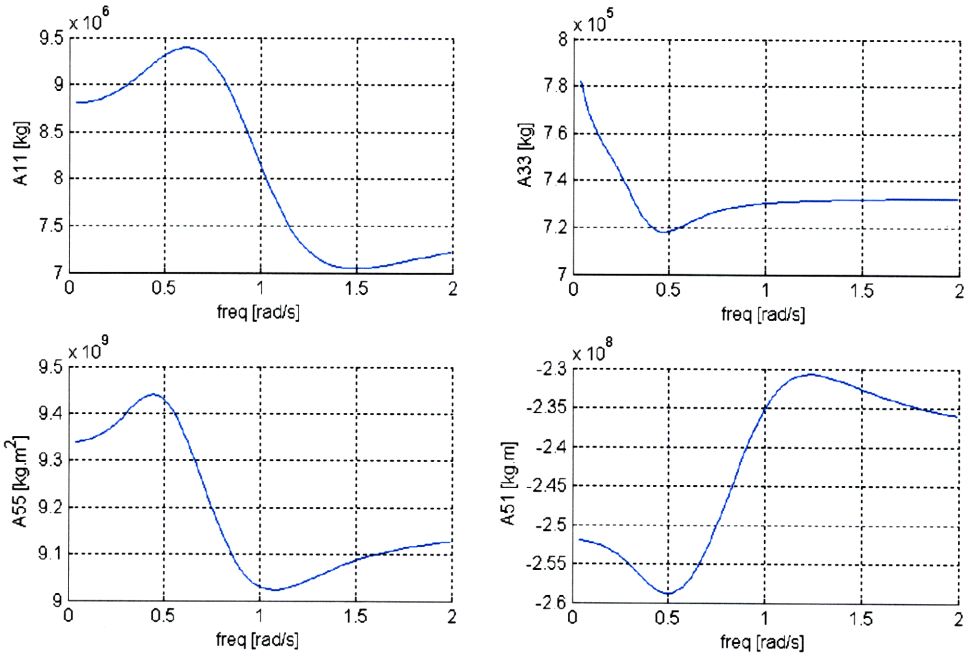

Figure2. Added mass coefficients

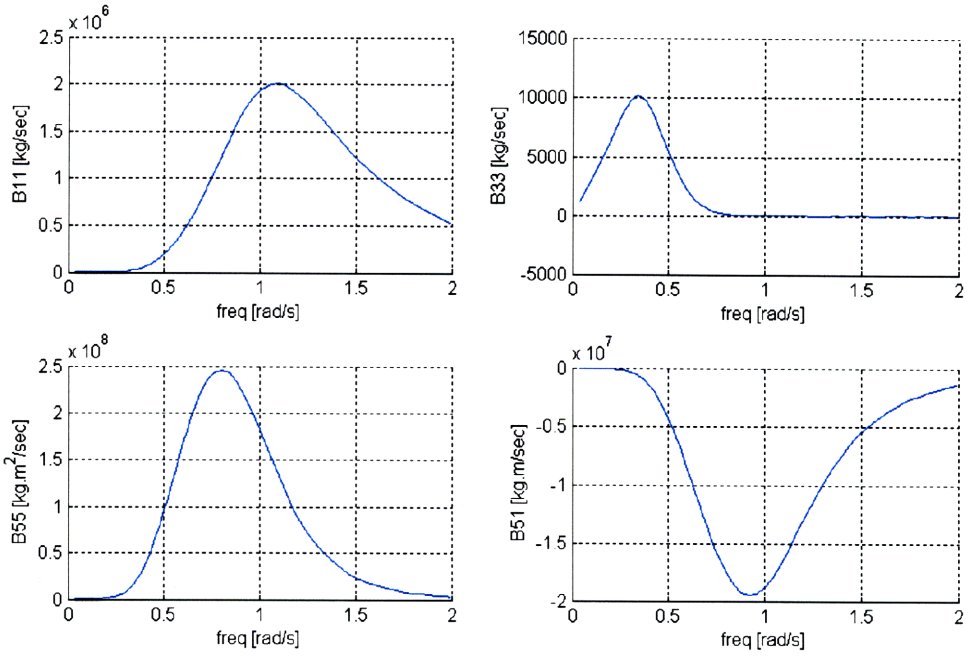

Figure3. Damping coefficients

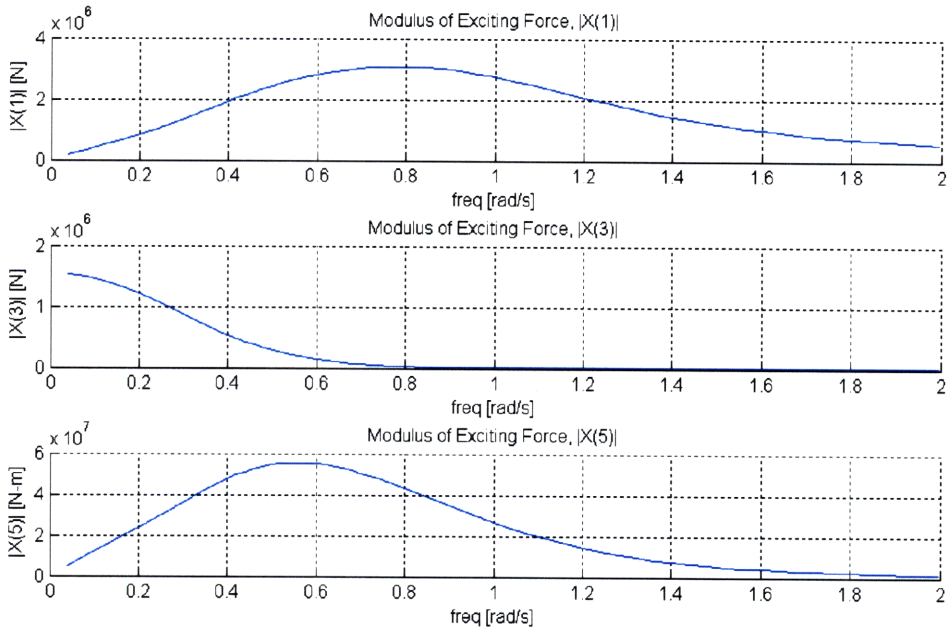

Figure4. Exciting forces

2.3. The Floating Wind Turbine System

The basis specification for the entire floating wind turbine platform has been tabulated as shown below. This is a particular platform design that is being uniformly used as the basis platform during the entire analysis of the present paper.

Properties		As-designed	Units
Platform	Diameter	14	M
	Draft	60	M
	Displacement	9485.66	metric tons
Concrete ballast	Concrete mass	8042.43	metric tons
	Concrete height	20.38	M
Water depth		150	M
Wind turbine mass		700	metric tons
Steel mass		745	metric tons
Center of gravity	X	0	M
	Y	0	M
	Z	-39.68	M

Table2. The structural property of the entire floating wind turbine platform

2.4. The Equation of Motions

The equations of motion for the entire system can be expressed in a 3-dimensional matrix form as shown below.

$$M(w)\ddot{\xi}(t) + B(w)\dot{\xi}(t) + C\xi(t) = aX(w)e^{iwt}$$

$M(w)$ = Total mass matrix [6x6]
$B(w)$ = Total damping matrix [6x6]
C = Total stiffness matrix [6x6]
$X(w)$ = Vector of wave induced exciting forces and moments [6x1]
$\xi(t)$ = Vector of system's displacement [6x1]
$\dot{\xi}(t)$ = Vector of system's velocity [6x1]
$\ddot{\xi}(t)$ = Vector of system's acceleration [6x1]
w = Incident wave frequency

The total mass, damping, and stiffness matrix consists of the components as shown below.

$$M(w) = M_{platform} + M_{windturbine} + M_{added}(w)$$
$$B(w) = B_{windturbine} + B_{platform}(w)$$
$$C = C_{platform} + C_{windturbine} + C_{mooring}$$

$M_{added}(w)$ = Added mass matrix [6x6]
$B_{platform}(w)$ = Wave damping matrix [6x6]

Once the basis system design was selected, the corresponding dynamic properties have been accurately evaluated based on pre-developed numerical analysis codes

including WAMIT and LINES, which were developed at MIT LSPF (MIT Laboratory for Ships and Platform Flows). The table shows the methods that have been used to evaluate those dynamic properties.

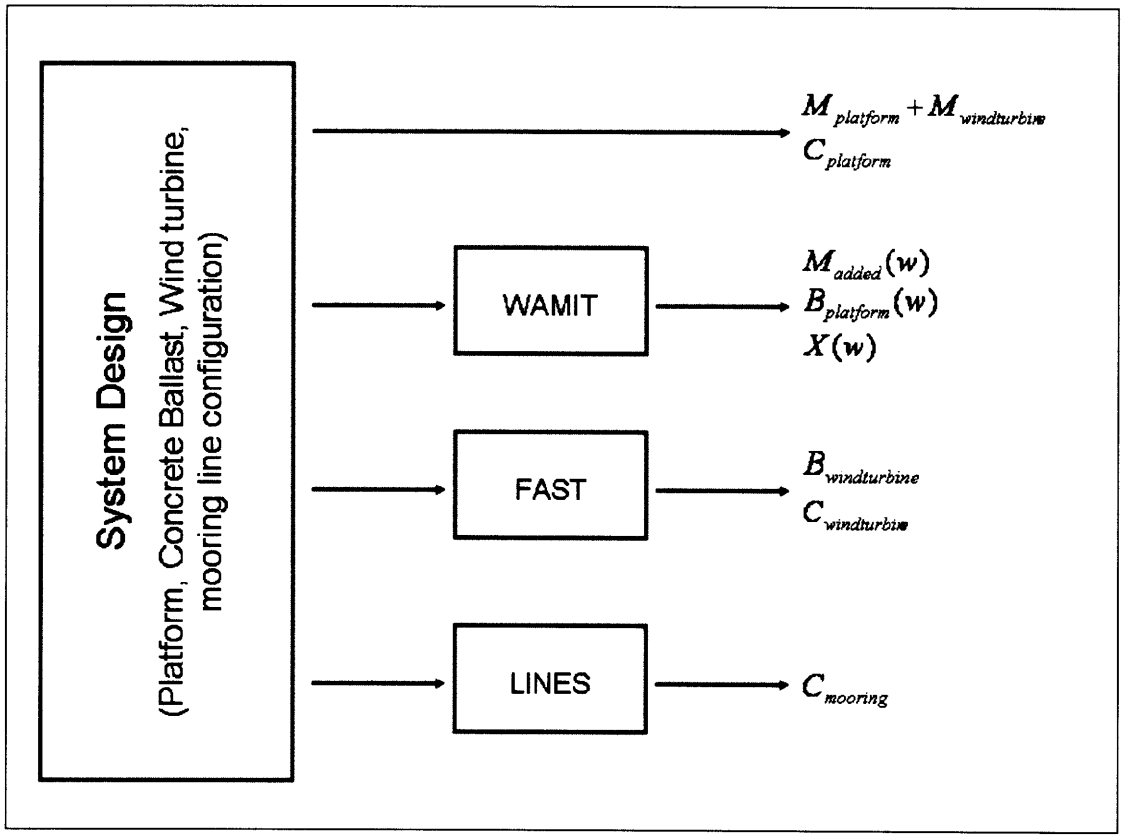

Figure5. The system property evaluations by numerical codes

Since the wave induced pressure field and its resultant exciting force acting on the platform oscillate as a function of time, each mode of motion becomes a sinusoidal function of time as well. It can be expressed in a complex form and substituted back to the equation of motion as shown below so as to achieve the system response in a frequency domain.

$$\xi(t) = \mathrm{Re}\{\Xi e^{iwt}\}$$

$$-w^2 M(w)\Xi e^{iwt} + iwB(w)\Xi e^{iwt} + C\Xi e^{iwt} = Xe^{iwt}$$

$$[-w^2 M(w) + iwB(w) + C]\Xi e^{iwt} = Xe^{iwt}$$

$$\Xi(w) = [-w^2 M(w) + iwB(w) + C]^{-1} X(w)$$

Accordingly, the entire system response in a frequency domain can be expressed in a matrix form as shown below.

$$\begin{pmatrix} RAO1(w) \\ RAO2(w) \\ RAO3(w) \\ RAO4(w) \\ RAO5(w) \\ RAO6(w) \end{pmatrix} = [-w^2 M(w) + iwB(w) + C]^{-1} \begin{pmatrix} X1(w) \\ X2(w) \\ X3(w) \\ X4(w) \\ X5(w) \\ X6(w) \end{pmatrix}$$

The six modes of motion including the incident wave and wind direction that are being used on the present paper follow a definition illustrated below.

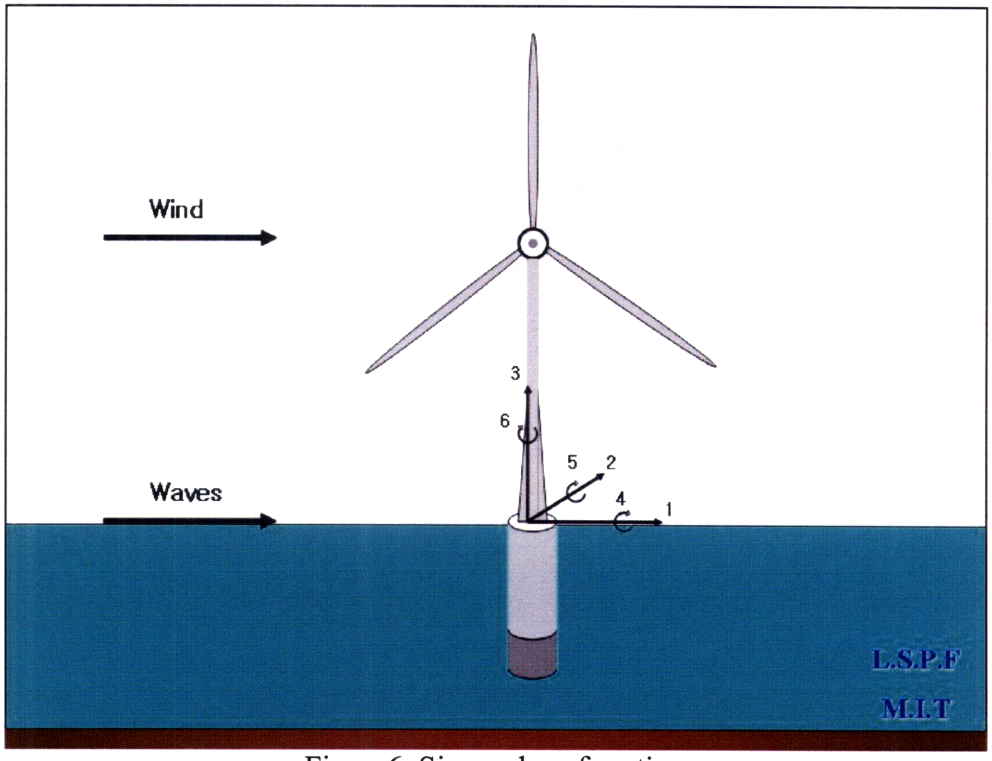

Figure6. Six modes of motion

2.5. Sea States and RMS Values

For open sea conditions the ISSC (International Ship Structures Committee) and the ITTC (International Towing Tank Conference) recommended the use of the following spectral density function:[1]

$$S(w) = H_s{}^2 T_1 \frac{0.11}{2\pi}\left(\frac{wT_1}{2\pi}\right)^{-5} e^{-0.44\left(\frac{wT_1}{2\pi}\right)^{-4}}$$

H_s = Significant wave height defined as the mean of the 1/3 highest waves

T_1 = Mean wave period in the above spectral density function

Based on the theory of linear wave induced motion, standard deviations from the mean value can be evaluated by the equation shown below. This value is being referred to RMS (root mean square) value at the present paper.

$$\sigma_i^{\,2} = \int_0^{\infty} RAO_i(w)^2 S(w) dw$$

2.6. Design Constraints

There are several particular requirements and constraints on the current floating wind turbine system design. The detailed explanation for these can be found in the paper by Chris Tracy [Reference 4]. Some of the designs that are being used on catenary design comparisons which are at chapter 5 might not necessarily satisfy all those conditions, however those are fully taken account for during the Pareto fronts simulation in the last chapter.

Design Constraints	Requirements	Units
Towing stability, $C_{withoutMooring_{5,5}}$	> 7.0E07	N-m/rad
Operating stability, $C_{total_{5,5}}$	>4.2E08	N-m/rad
Maximal dynamic pitch, $\xi_5 + \sigma_{\xi_5}$	<10	Degree
Maximum line tension, $T_{mean} + 3\sigma$	<MBL	Metric tons
Slamming	>0	M
Nacelle acceleration	<0.3	G

Table3. Operational basis design requirements for floating wind turbines

[1] Sclavounos, P. D., *Surface Waves and Their Interaction with Floating Bodies, Lecture Notes,* Massachusetts Institute of Technology, Cambridge, MA

3. Design Parameters

For each type of catenary mooring line design, the sensitivity analysis has been performed varying the parameters such as the angle of catenary at anchor, the characteristic length of catenary (or pretension on catenary), or the fairlead location in order to find out a reasonable combination of those that can possibly get the entire dynamic performances optimized as the best. All of the design analysis until chapter 5 is based on the water depth of 150m. The definitions of each parameter are listed below.

Fairlead Location, L

$$L = \frac{\text{Depth of Fairlead}}{\text{Platform Draft}}$$

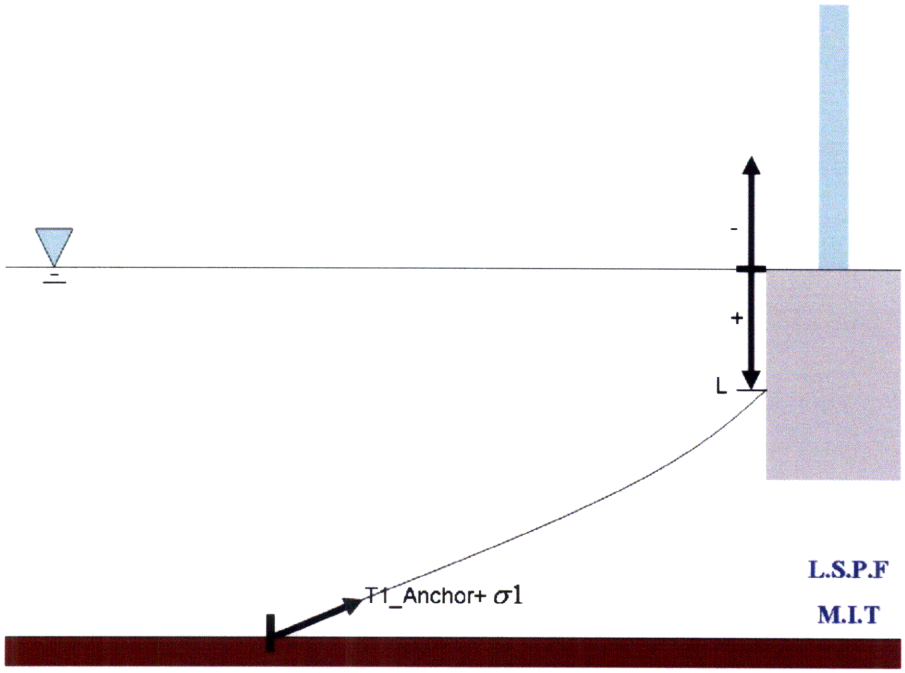

Figure7. The definition of L

Angle of Catenary at Anchor, Alpha

Alpha = Catenary Angle from the Seabed

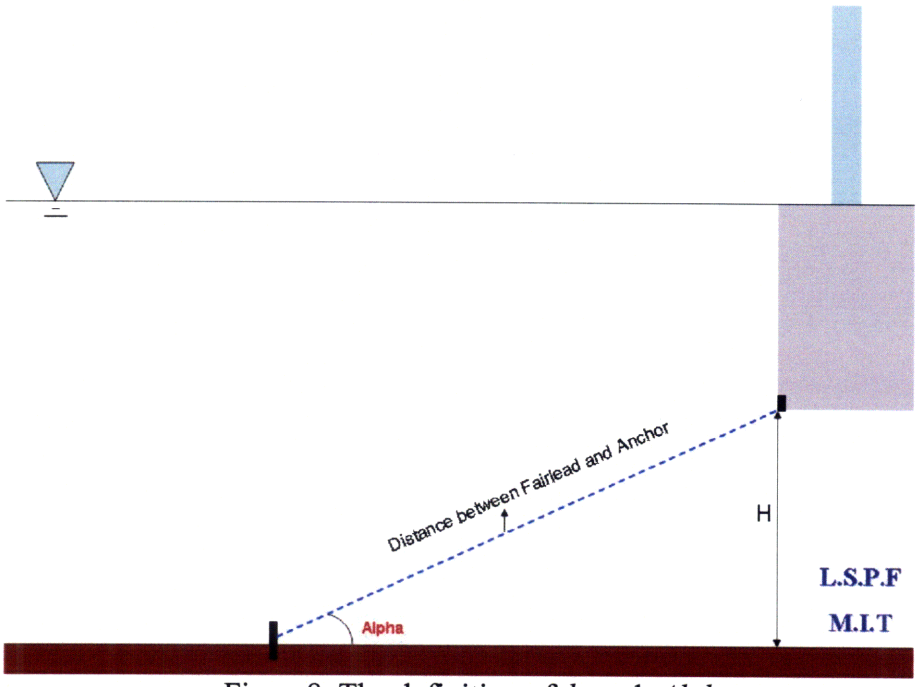

Figure8. The definition of k and *Alpha*

Characteristic Length of Catenary, k

$$k = \frac{\text{Unstretched Original Length of Catenary}}{\text{Distance between Fairlead and Anchor}}$$

The characteristic length of catenary, k can be expressed as shown below.

$$k = \frac{L_o}{\sqrt{H^2 + (\frac{H}{\tan\alpha})^2}}$$

Where, L_o = unstretched original length of catenary
H = height of the bottom of buoy

The pretension, T_{pre} applied to a catenary can be then expressed as a function of characteristic length of carenary, k as shown below.

$$\begin{aligned} T_{pre} &= EA \cdot \frac{\Delta L}{L_o} \\ &= EA \cdot \frac{\Delta L}{L_o} \\ &= EA \cdot \frac{\sqrt{H^2 + (\frac{H}{\tan\alpha})^2} - L_o}{L_o} \\ &= EA \cdot \frac{\sqrt{H^2 + (\frac{H}{\tan\alpha})^2} - k \cdot \sqrt{H^2 + (\frac{H}{\tan\alpha})^2}}{k \cdot \sqrt{H^2 + (\frac{H}{\tan\alpha})^2}} \\ &= EA\frac{1-k}{k} \end{aligned}$$

Where, E = Elastic modulus of catenary
A = Cross sectional area of catenary
k = Characteristic length of catenary

Maximum Breaking Load, MBL

MBL is the specified minimum breaking load of the mooring line, and can be expressed as shown below.[2]

[2] N.F. Casey, Tuvnel, S.J. Banfield, TTI, "Factors Affecting Measurement of Axial Stiffness of Polyester Deepwater Mooring Rope Under Sinusoidal Loading", *Offshore Technology Conference,* May, 2005

$$MBL = \frac{EA}{K_{rd}}$$

Where, E = Elastic modulus of catenary

A = Cross sectional area of catenary

K_{rd} = 20, Dynamic Axial Stiffness

In the DLC (Double Layered Catenary) mooring system, the MBL has been designed to be equal on both layers as shown below.

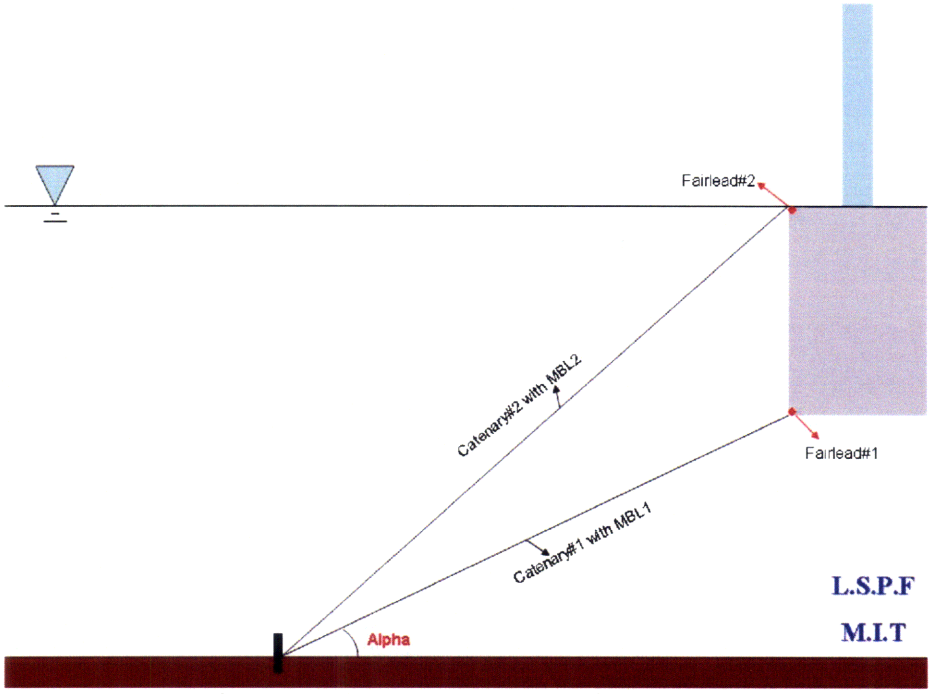

Figure9. MBL's on DLC mooring system

4. Basis Design Analysis

4.1. SLC (Single-Layered Catenary)

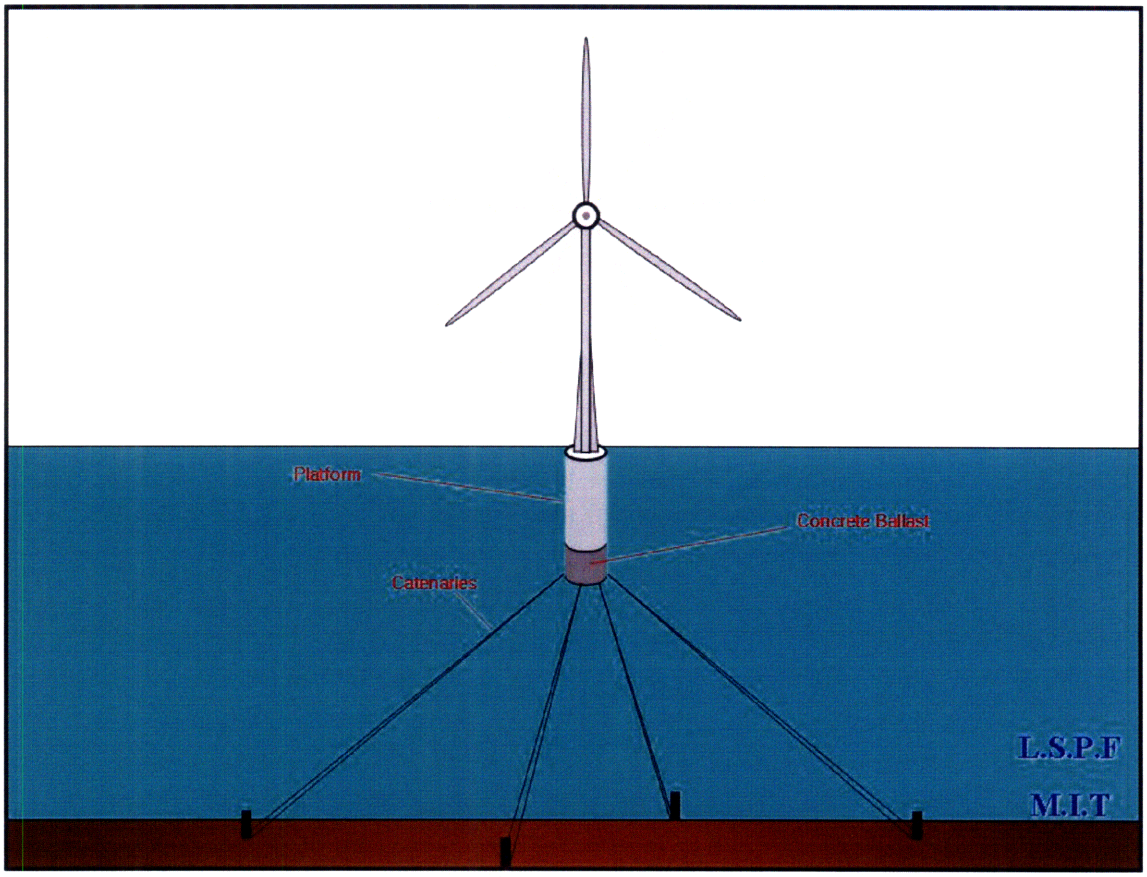

Figure10. SLC

4.1.1. When k = 0.990 m/m, T_{pre} =2E6 N

4.1.1.1. Specifications

Properties		Values		
Platform	Diameter [m]		14	
	Draft [m]		60	
	Displacement [metric tons]		9485.66	
Concrete	Concrete Mass [metric tons]		8042.43	
	Concrete Height [m]		20.38	
Center of Gravity [m]			-39.68	
Center of Buoyancy [m]			-30	
Sea condition	Water depth [m]		150	
Mooring	Alpha [degree]	Varies	Minimum	Maximum
			30	75
	k [m/m]		0.990	
	Fairlead Location, L [m/m]		1	
	* EA [N]		200E6	
	Pretension, T_{pre} [N]		2E6	
	MBL [N]		10E6	

* EA = $K_{rd} \times MBL$ (E: the catenary modulus, EA: the gradient of loading, K_{rd} : the dynamic axial stiffness, MBL: the minimum breaking load of the catenary)

4.1.1.2. Dynamic Performances

The system dynamic behaviors in each RMS value have been evaluated varying the catenary angle from sea bed, and been plotted below.

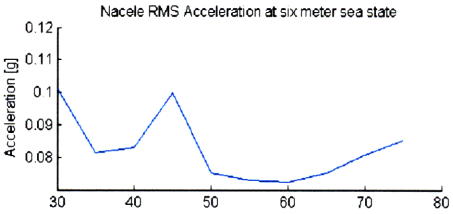

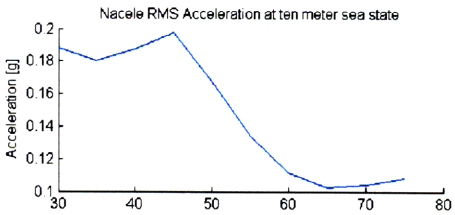

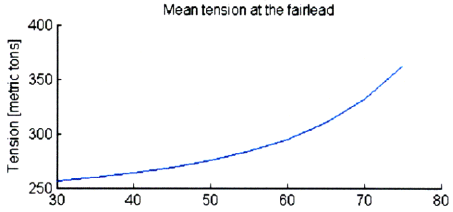

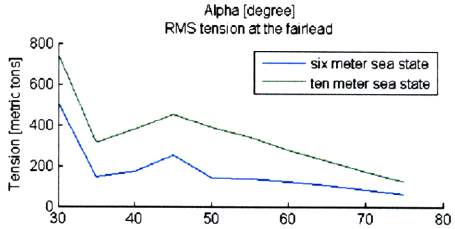

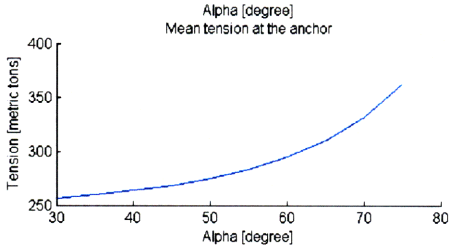

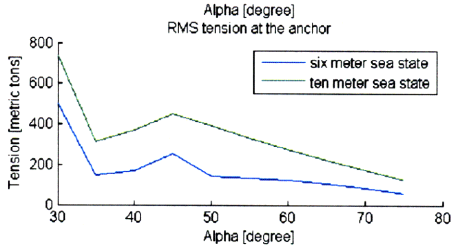

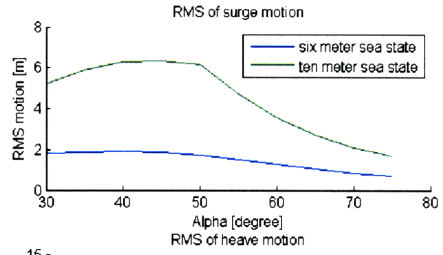

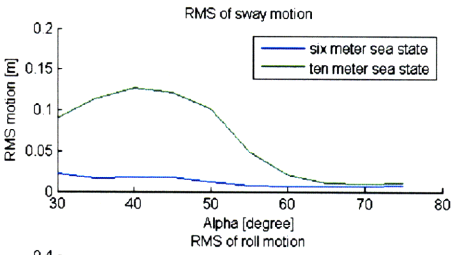

The RAO for three different angles have been evaluated and compared as shown below.

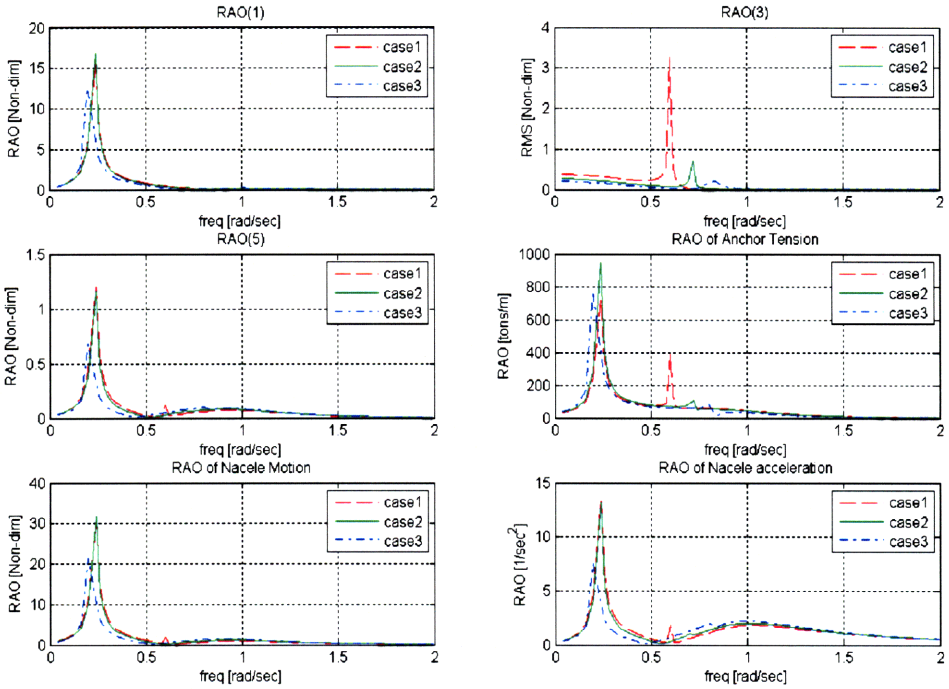

(Case1: Alpha=40; Case2: Alpha=50; Case3: Alpha=60)

4.1.2. When k = 0.985 m/m, T_{pre} =3E6 N

4.1.2.1. Specifications

Properties		Values		
Platform	Diameter [m]		14	
	Draft [m]		60	
	Displacement [metric tons]		9485.66	
Concrete	Concrete Mass [metric tons]		8042.43	
	Concrete Height [m]		20.38	
Center of Gravity [m]			-39.68	
Center of Buoyancy [m]			-30	
Sea condition	Water depth [m]		150	
Mooring	Alpha [degree]	Varies	Minimum	Maximum
			30	75
	k [m/m]		0.985	
	Fairlead Location, L [m/m]		1	
	* EA [N]		200E6	
	Pretension, T_{pre} [N]		3E6	
	MBL [N]		10E6	

* EA = $K_{rd} \times MBL$ (E: the catenary modulus, EA: the gradient of loading, K_{rd} : the dynamic axial stiffness, MBL: the minimum breaking load of the catenary)

4.1.2.2. Dynamic Performances

The system dynamic behaviors in each RMS value have been evaluated varying the catenary angle from sea bed, and been plotted below.

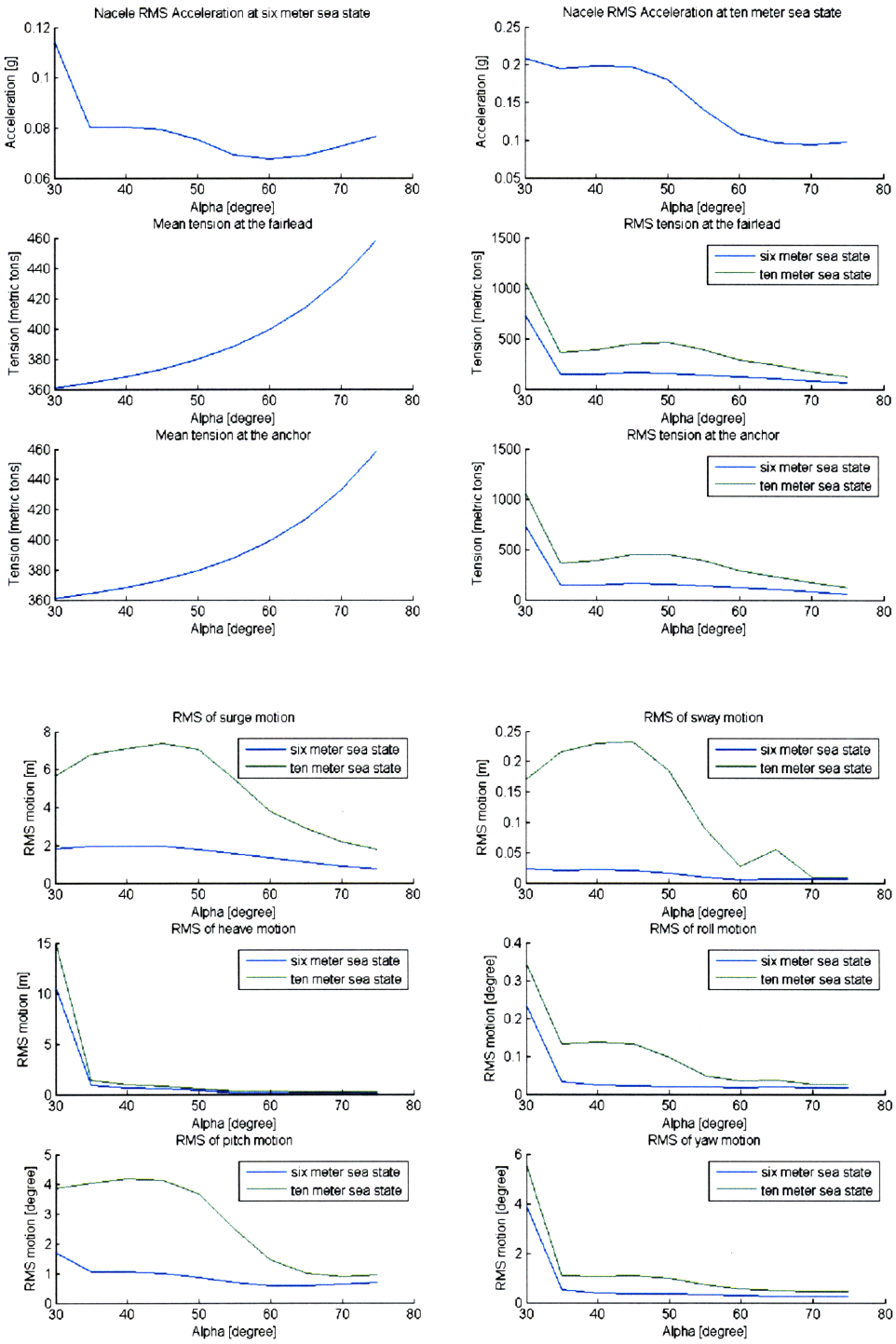

The RAO for three different angles have been evaluated and compared as shown below.

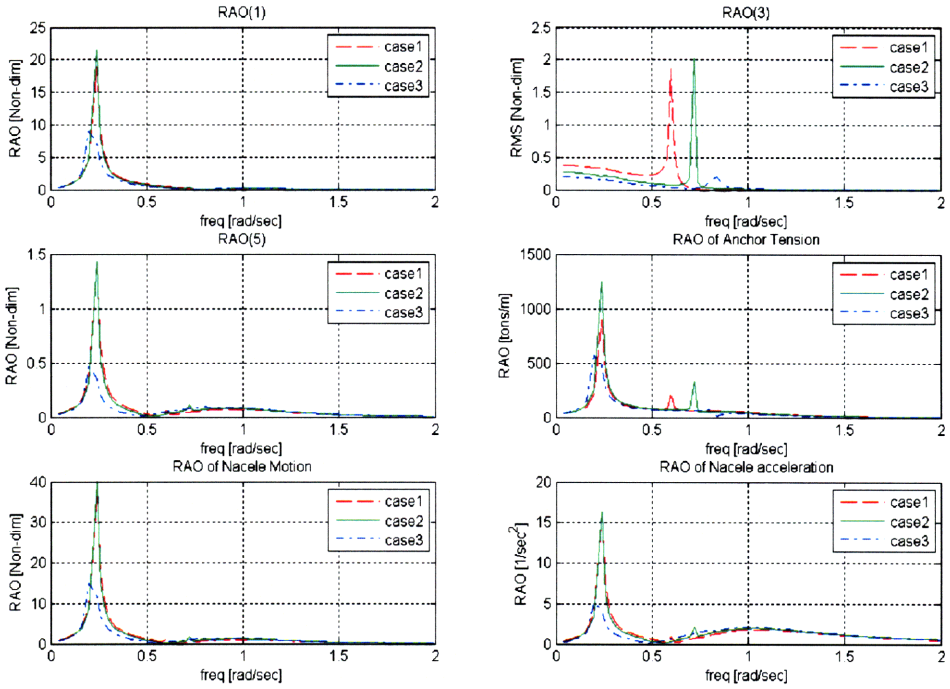

(Case1: Alpha=40; Case2: Alpha=50; Case3: Alpha=60)

4.2. BSLC (Ballasted Single-Layered Catenary)

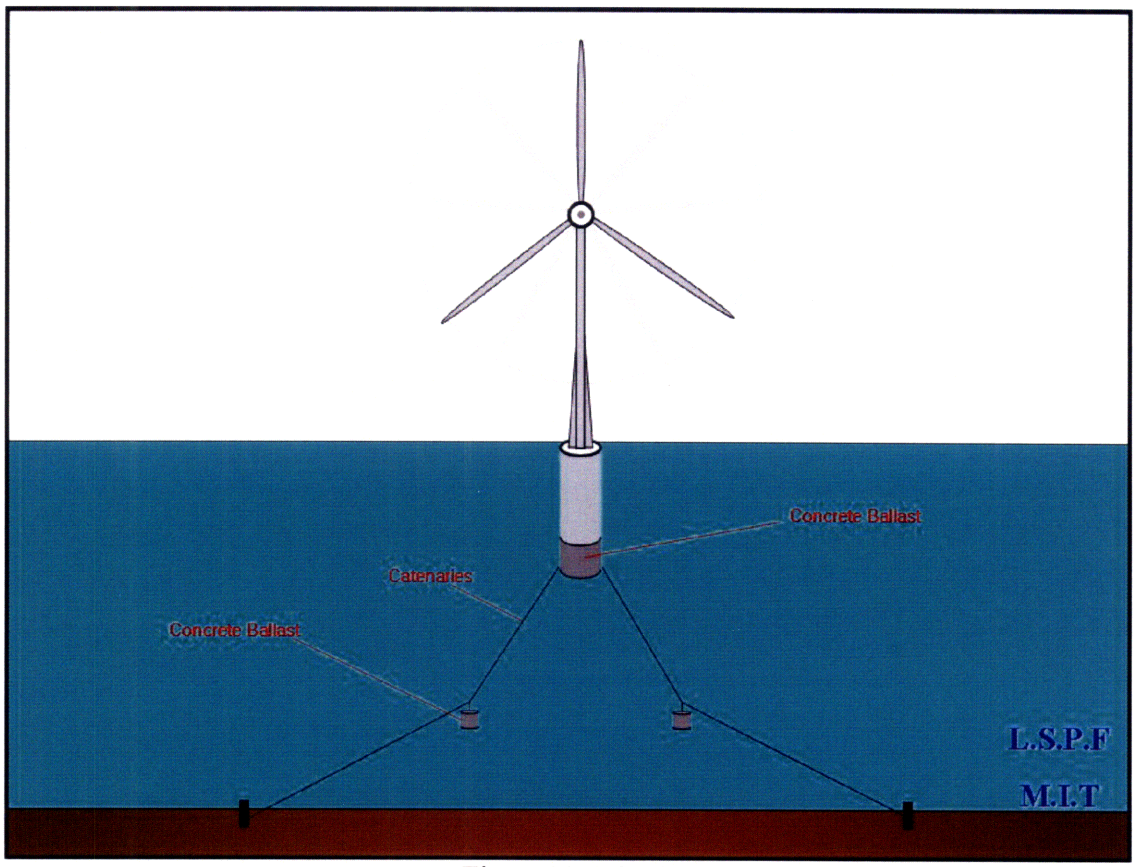

Figure11. BSLC

4.2.1. When k = 0.990 m/m, T_{pre} =2E6 N

4.2.1.1. Specifications

Properties		Values		
Platform	Diameter [m]		14	
	Draft [m]		60	
	** Displacement [metric tons]		9485.66	
Concrete	Concrete Mass [metric tons]		8042.43	
	Concrete Height [m]		20.38	
Center of Gravity [m]			-39.68	
Center of Buoyancy [m]			-30	
Sea condition	Water depth [m]		150	
Mooring	Alpha [degree]	Varies	Minimum	Maximum
			30	75
	k [m/m]		0.990	
	Fairlead Location, L [m/m]		1	
	* EA [N]		200E6	
	Pretension, T_{pre} [N]		2E6	
	MBL [N]		10E6	
	Concrete Ballast Mass per line [metric tons]		70	

* EA = $K_{rd} \times MBL$ (E: the catenary modulus, EA: the gradient of loading, K_{rd} : the dynamic axial stiffness, MBL: the minimum breaking load of the catenary)
**Note: the corresponding effects on system displacement due to the concrete ballast mass is ignored during the present analysis

4.2.1.2. Dynamic Performances

The system dynamic behaviors in each RMS value have been evaluated varying the catenary angle from sea bed, and been plotted below.

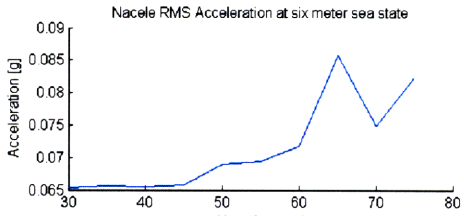

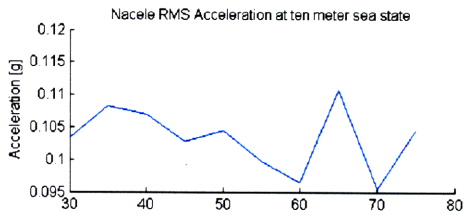

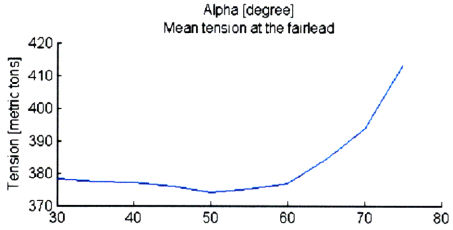

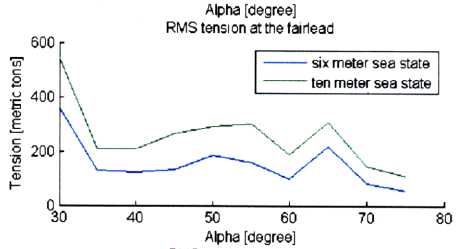

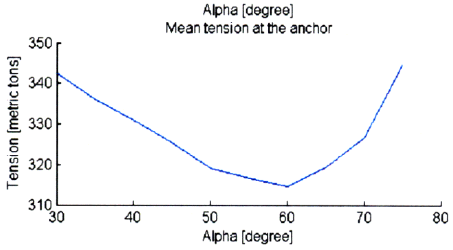

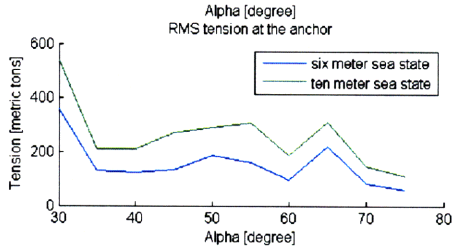

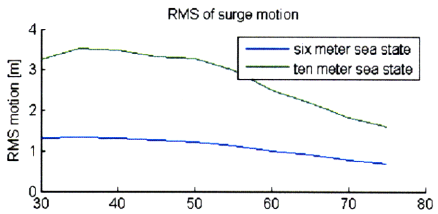

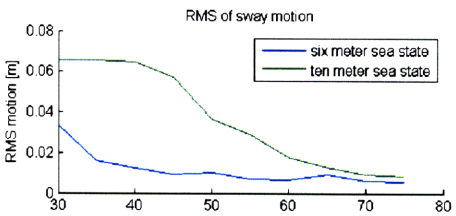

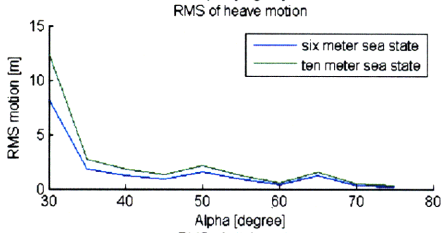

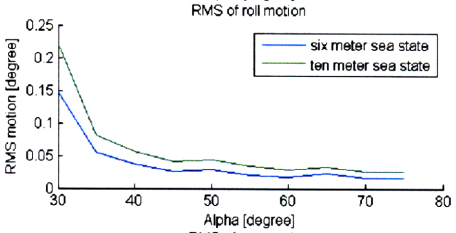

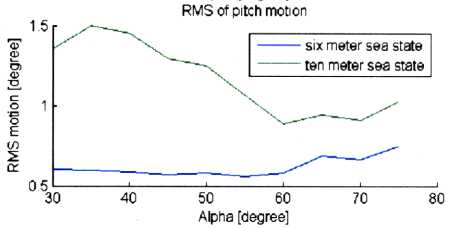

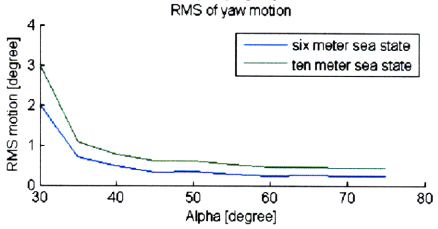

The RAO for three different angles have been evaluated and compared as shown below.

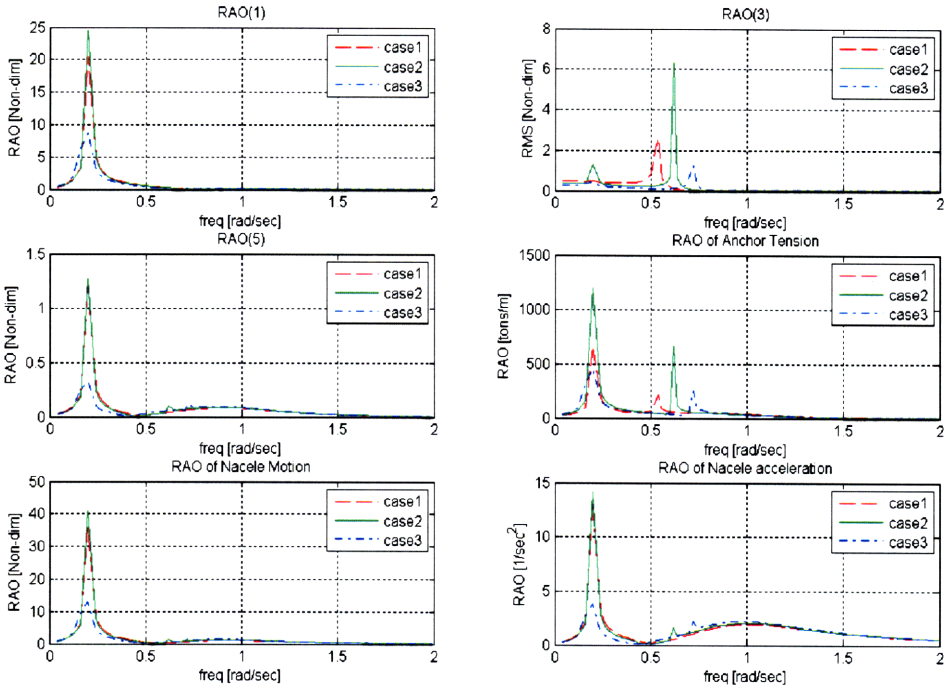

(Case1: Alpha=40; Case2: Alpha=50; Case3: Alpha=60)

4.2.2. When k = 0.985 m/m, T_{pre} =3E6 N

4.2.2.1. Specifications

Properties		Values		
Platform	Diameter [m]		14	
	Draft [m]		60	
	** Displacement [metric tons]		9485.66	
Concrete	Concrete Mass [metric tons]		8042.43	
	Concrete Height [m]		20.38	
Center of Gravity [m]			-39.68	
Center of Buoyancy [m]			-30	
Sea condition	Water depth [m]		150	
Mooring	Alpha [degree]	Varies	Minimum	Maximum
			30	75
	k [m/m]		0.985	
	Fairlead Location, L [m/m]		1	
	* EA [N]		200E6	
	Pretension, T_{pre} [N]		3E6	
	MBL [N]		10E6	
	Concrete Ballast Mass per line [metric tons]		70	

* EA = $K_{rd} \times MBL$ (E: the catenary modulus, EA: the gradient of loading, K_{rd} : the dynamic axial stiffness, MBL: the minimum breaking load of the catenary)
**Note: the corresponding effects on system displacement due to the concrete ballast mass is ignored during the present analysis

4.2.2.2. Dynamic Performances

The system dynamic behaviors in each RMS value have been evaluated varying the catenary angle from sea bed, and been plotted below.

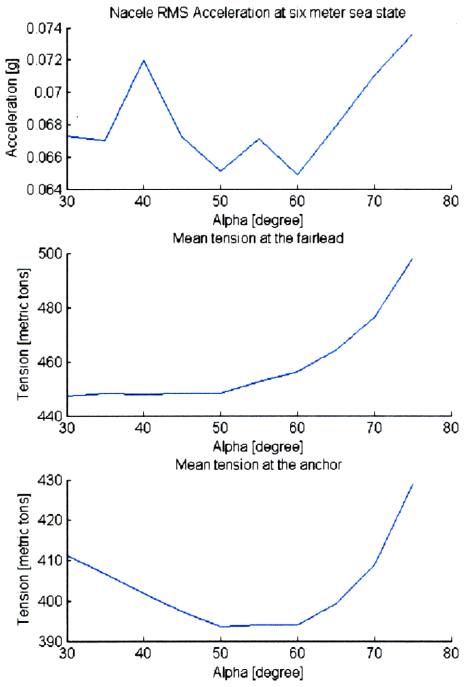

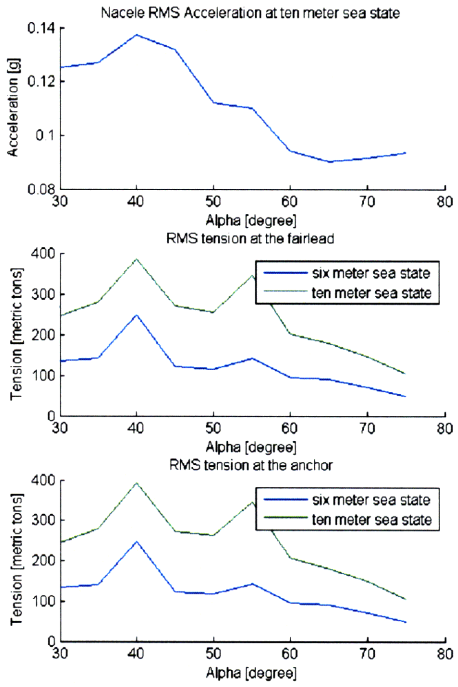

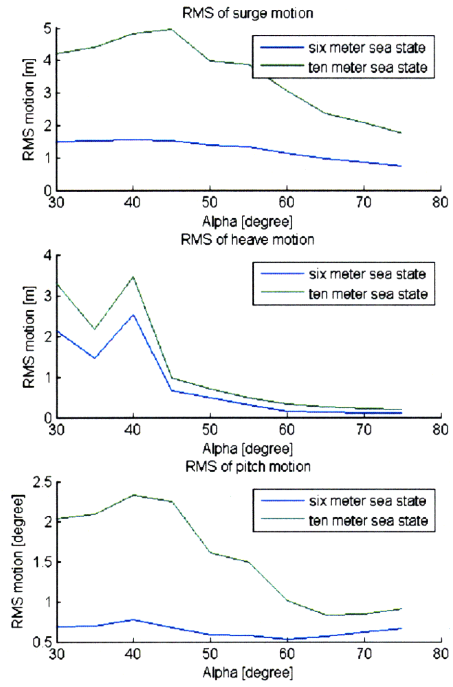

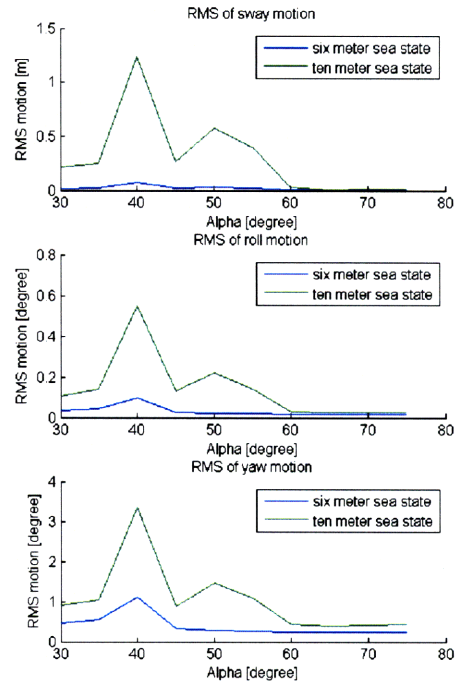

The RAO for three different angles have been evaluated and compared as shown below.

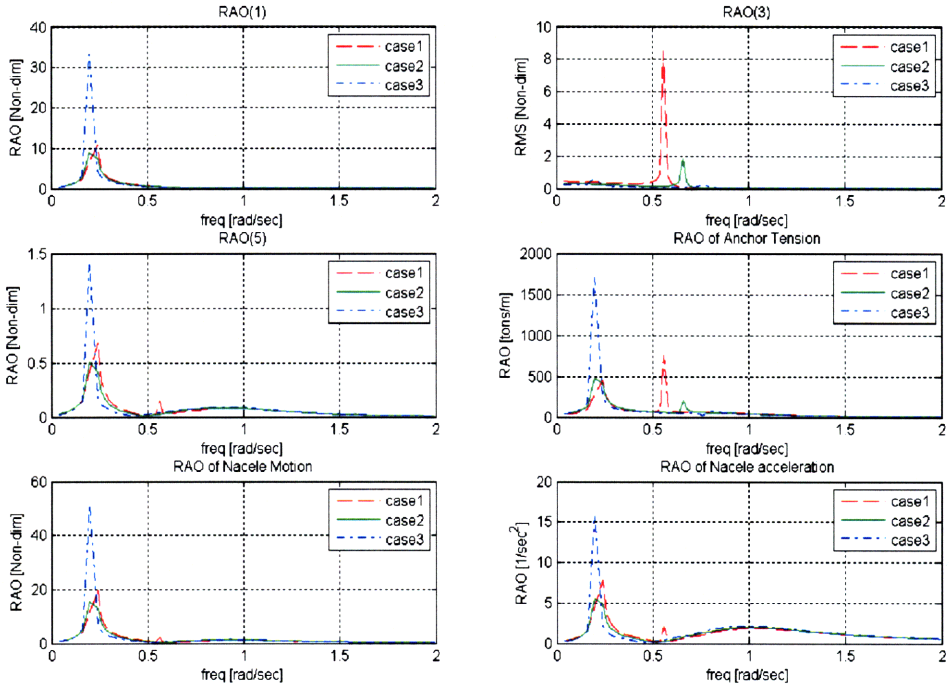

(Case1: Alpha=40; Case2: Alpha=50; Case3: Alpha=60)

4.3. Comparison of SLC and BSLC

4.3.1. When Alpha = 60 deg, k = 0.990 m/m, T_{pre} =2E6 N

4.3.1.1. SLC

Sea States, Hs		6m	10m	Units
RMS Nacelle Acceleration		0.072	0.112	g
RMS Motions	Surge	1.268	3.562	m
	Heave	0.126	0.258	m
	Pitch	0.629	1.429	degree
*Fairlead Tension	Mean	294.903	294.903	metric tons
	RMS	120.784	276.998	metric tons
*Anchor Tension	Mean	294.699	294.699	metric tons
	RMS	120.946	275.513	metric tons

(*All of the tension components are picked up from windward side)

Table8. SLC with k=0.990

4.3.1.2. BSLC with suspension ballast of 70 metric tons

Sea States, Hs		6m	10m	Units
RMS Nacelle Acceleration		0.072	0.096	g
RMS Motions	Surge	0.996	2.488	m
	Heave	0.339	0.533	m
	Pitch	0.582	0.890	deg
*Fairlead Tension	Mean	376.889	376.889	metric tons
	RMS	97.781	189.319	metric tons
*Anchor Tension	Mean	314.686	314.686	metric tons
	RMS	97.135	185.437	metric tons

(*All of the tension components are picked up from windward side)

Table9. BSLC with k=0.990

As seen in the above table, a ballasted catenary induces a higher mean tension on the line as it's supposed to be. However, the RMS tension decreases a lot, and therefore the

effective total tension acting on the lines is significantly decreasing down especially at ten meter sea state.

4.3.2. When Alpha = 60 deg, k = 0.985 m/m, T_{pre} =3E6 N

4.3.2.1. SLC

Sea States, Hs		6m	10m	Units
RMS Nacelle Acceleration		0.068	0.108	g
RMS Motions	Surge	1.306	3.787	m
	Heave	0.122	0.254	m
	Pitch	0.584	1.431	degree
*Fairlead Tension	Mean	398.914	398.914	metric tons
	RMS	121.188	289.135	metric tons
*Anchor Tension	Mean	398.711	398.711	metric tons
	RMS	121.188	289.135	metric tons

(*All of the tension components are picked up from windward side)

Table10. SLC with k=0.985

4.3.2.2. BSLC with suspension ballast of 70 metric tons

Sea States, Hs		6m	10m	Units
RMS Nacelle Acceleration		0.065	0.094	g
RMS Motions	Surge	1.142	3.056	m
	Heave	0.155	0.312	m
	Pitch	0.524	1.010	deg
*Fairlead Tension	Mean	456.019	456.019	metric tons
	RMS	93.689	200.204	metric tons
*Anchor Tension	Mean	394.020	394.020	metric tons
	RMS	95.675	205.871	metric tons

(*All of the tension components are picked up from windward side)

Table11. BSLC with k=0.985

4.3.3. When Alpha = 50 deg, k = 0.990 m/m, T_{pre}=2E6 N

4.3.3.1. SLC

Sea States, Hs		6m	10m	Units
RMS Nacelle Acceleration		0.075	0.167	g
RMS Motions	Surge	1.723	6.150	m
	Heave	0.220	0.401	m
	Pitch	0.845	3.286	degree
*Fairlead Tension	Mean	275.120	275.120	metric tons
	RMS	140.905	389.949	metric tons
*Anchor Tension	Mean	274.917	274.917	metric tons
	RMS	140.905	389.949	metric tons

(*All of the tension components are picked up from windward side)

Table12. SLC with k=0.990

4.3.3.2. BSLC with suspension ballast of 120 metric tons

Sea States, Hs		6m	10m	Units
RMS Nacelle Acceleration		0.064	0.093	g
RMS Motions	Surge	1.128	2.885	m
	Heave	0.868	1.242	m
	Pitch	0.524	0.993	deg
*Fairlead Tension	Mean	455.815	455.815	metric tons
	RMS	113.566	194.108	metric tons
*Anchor Tension	Mean	361.389	361.389	metric tons
	RMS	112.416	189.024	metric tons

(*All of the tension components are picked up from windward side)

Table13. BSLC with k=0.990

4.3.4. When Alpha = 50 deg, suspension ballast = 120 metric tons, k = 0.985 m/m, T_{pre} =3E6 N

4.3.4.1. SLC

Sea States, Hs		6m	10m	Units
RMS Nacelle Acceleration		0.075	0.180	g
RMS Motions	Surge	1.774	7.056	m
	Heave	0.393	0.575	m
	Pitch	0.848	3.680	degree
*Fairlead Tension	Mean	379.744	379.744	metric tons
	RMS	155.989	465.684	metric tons
*Anchor Tension	Mean	379.540	379.540	metric tons
	RMS	152.966	451.923	metric tons

(*All of the tension components are picked up from windward side)

Table14. SLC with k=0.985

4.3.4.2. BSLC with suspension ballast of 120 metric tons

Sea States, Hs		6m	10m	Units
RMS Nacelle Acceleration		0.063	0.109	g
RMS Motions	Surge	1.366	4.008	m
	Heave	0.477	0.752	m
	Pitch	0.560	1.557	deg
*Fairlead Tension	Mean	521.281	521.281	metric tons
	RMS	103.534	243.010	metric tons
*Anchor Tension	Mean	427.059	427.059	metric tons
	RMS	103.534	243.010	metric tons

(*All of the tension components are picked up from windward side)

Table15. BSLC with k=0.985

In the case of 50 deg catenary angle, and 120 tons suspension concrete ballast, the ballasted catenary effect becomes more significant as seen in the above table. At the ten meter sea state with k of 0.990 m/m, the mean tension increases by 80 tons which is

obvious, but the corresponding RMS tension decreases by 200 tons. In addition to that, the angle of catenary at anchor also decreases to 44.4 deg, which is smaller than before as well.

4.3.5. Comparison in RAO

The RAOs in surge, heave, pitch, and anchor tension have been plotted and compared at two different types of catenary mooring systems, the original regular cateanry and the ballasted catenary respectively.

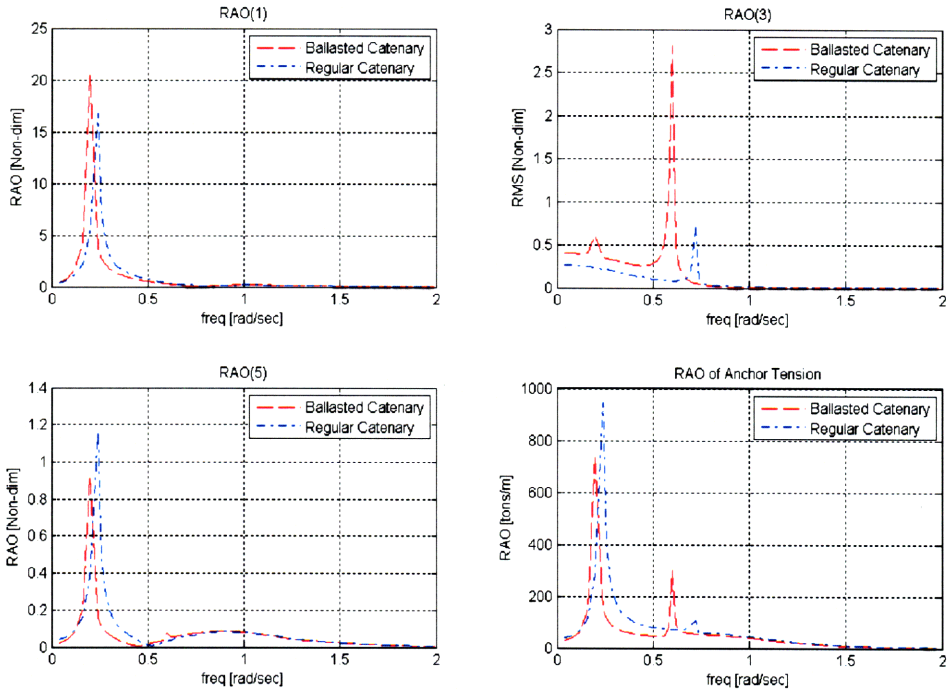

Figure12. The RAOs by ballasted catenary (70 metric tons) and regular catenary mooring system when alpha = 50 deg, k = 0.990 m/m

As shown on the plots above, the resonant frequency shifts significantly lower by suspending a ballast mass at catenary line. The RAO peak at resonant frequency is increased in surge and heave motion, but it's decreased a bit in pitch motion. The tension at the anchor is a function of motion responses, and therefore the peaks at tension RAO also decrease.

The spectral density functions for six and ten meter sea states have a peak spreading from 0.2 through 0.4 rad/sec. The plot of RAO of anchor tension shown above reveals that the total overlapping between the RAO and sea spectrum is getting decreased a bit due to the

huge vacancy made by the first peak near sea spectrum even though the second peak is getting closer to the sea spectrum. This is the reason why the RMS tension at the anchor is decreasing especially at the ten meter sea state, which is one of the big advantages coming out of this ballasted catenary system.

The amount of effect due to the suspended ballast mass at catenary depends on the original configuration of mooring system, and this needs to be studied more thoroughly by parametric design process including Pareto optimization process in the future.

4.3.6. Comparison in Angle

As one of the advantages of ballasted catenary, the angle of catenary at anchor decreases down due to a ballast mass hang on the line. Most of the anchors being installed / used for offshore floating structures are relatively more vulnerable to vertical forces than to horizontal forces. Ballasted catenary provides a good solution to these systems in terms of having a smaller effective tension acting on the line and anchor, and having a smaller angle of catenary at anchor.

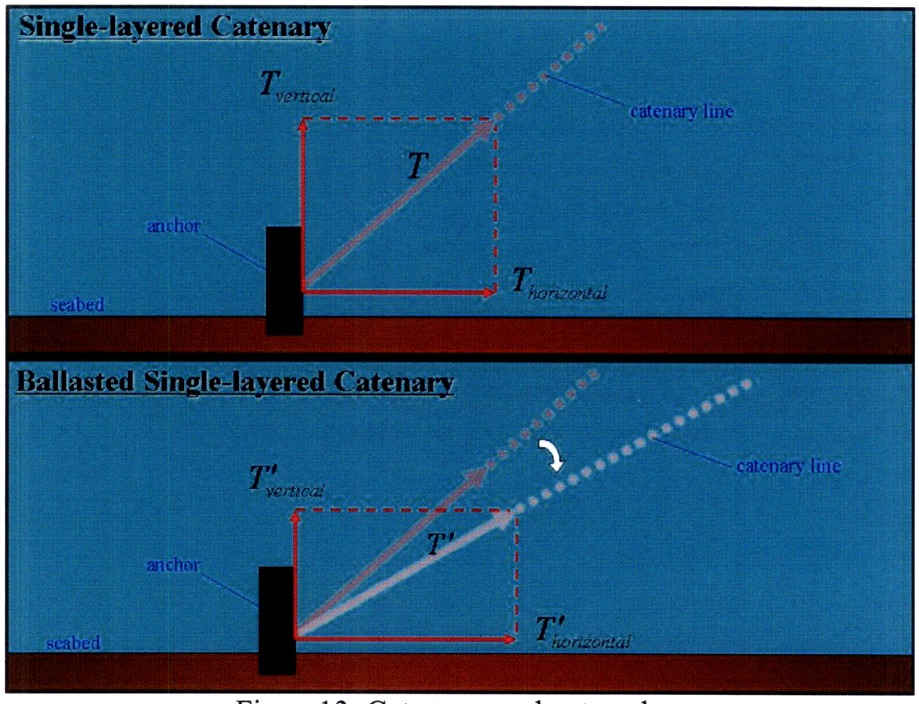

Figure13. Catenary angle at anchor

The anchor is loaded in horizontal and vertical direction. The type of anchor will be determined by the calculated maximum tensions / loads on the anchor with particular factor of safety, and by the type of soil in which it will be set.

$$T = \overline{T} + 4 \cdot \sigma_T$$

Where T =maximum anchor tension
$\overline{T}$ =mean anchor tension
σ_T =RMS anchor tension

$$T_{horizontal} = T \times \cos \alpha_{anchor}$$
$$T_{vertical} = T \times \sin \alpha_{anchor}$$

Where T =maximum anchor tension
α_{anchor} = angle of catenary at anchor
$T_{horizontal}$ =maximum horizontal anchor tension
$T_{vertical}$ =maximum vertical anchor tension

4.3.6.1. When Alpha = 60 deg, k = 0.990 m/m, T_{pre} =2E6 N

	SLC	BSLC	Units
Angle of Catenary at Fairlead	60.26	62.94	deg
Angle of Catenary at Anchor	60.24	57.01	deg

(*All of the tension components are picked up from windward side)

Table16. Angles of catenaries at the mean offset position when k=0.990

	SLC	BSLC	Units
Mean tension, $\overline{T}$	294.699	314.686	metric tons
RMS tension, σ_T	275.513	185.437	metric tons
Maximum tension, T	294+4*275=1394	314+4*185=1054	metric tons
Angle of catenary, α_{anchor}	60.24	57.01	deg
Maximum horizontal tension, $T_{horizontal}$	1394*cos60.24=691	1054*cos57.01=573	metric tons
Maximum vertical tension, $T_{vertical}$	1394*sin60.24=1210	1054*sin57.01=884	metric tons

(*All of the tension components are picked up from windward side)

Table17. Anchor tensions at 10 meter sea state

As seen in the above table, the effective maximum tension based on four sigma rule decreases by 340 tons from 1394 tons to 1054 tons. In addition, the angle of catenary at anchor decreases by 3 deg, and therefore the vertical tension component becomes smaller, which in this case is 884 tons for maxima.

4.3.6.2. When Alpha = 50 deg, k = 0.990 m/m, T_{pre} =2E6 N

	SLC	BSLC	Units
Angle of Catenary at Fairlead	50.29	55.48	deg
Angle of Catenary at Anchor	50.26	44.40	deg

(*All of the tension components are picked up from windward side)

Table18. Angles of catenaries at the mean offset position when k=0.990

	SLC	BSLC	Units
Mean tension, $\overline{T}$	274.917	361.389	metric tons
RMS tension, σ_T	389.949	189.024	metric tons
Maximum tension, T	274+4*389=1830	361+4*189=1117	metric tons
Angle of catenary, α_{anchor}	50.26	44.40	deg
Maximum horizontal tension, $T_{horizontal}$	1052*cos50.26=1169	739*cos44.40=798	metric tons
Maximum vertical tension, $T_{vertical}$	1052*sin50.26=1407	739*sin44.40=781	metric tons

(*All of the tension components are picked up from windward side)

Table19. Anchor tensions at 10 meter sea state

At the ten meter sea state with k of 0.990 m/m, the SLC and BSLC have been compared and tabulated above. The effective maximum tension based on four sigma rule decreases down by 713 tons from 1830 tons to 1117 tons. The angle of catenary at anchor decreases down by 6 deg, and therefore the effective total vertical tension component becomes smaller to 781 tons for maxima.

4.4. DLC (Double-Layered Catenary)

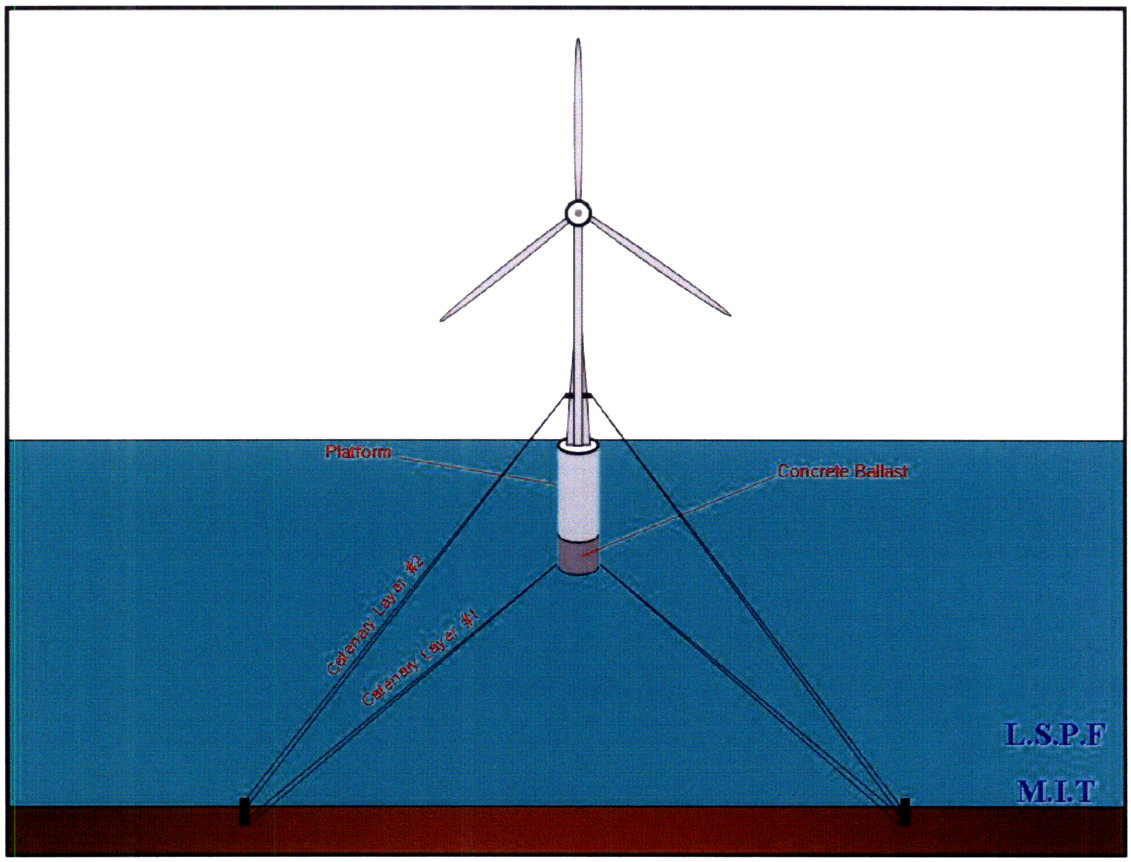

Figure14. DLC

4.4.1. Motivation

The majority of mooring systems on offshore floating structure such as oil rigs have been designed and applied primarily for station keeping, which prevents the structure from drifting away by ambient sea waves. Because of the higher inertia force due to the massive wind turbine structure at 64m above free surface, however, the system dynamic performances become significantly more sensitive to mooring line design compared to conventional offshore floating structures. The principal design purpose of mooring system on the present offshore structure is not only for the station keeping but also for the dynamic motion response control via affecting the system's dynamic properties such as stiffness, or etc. From this point of view, a double-layered catenary can potentially have a capability to provide an optimal restoring effect on the present offshore floating structure.

One of the requirements for the present design problem is to have the least number of anchorage installations. The original idea for a double-layered catenary came out of the dynamic response in pitch which I expected might be dominating over all other modes of motion in this system so as to have two separate tension components acting on an anchor out of phase from each other.

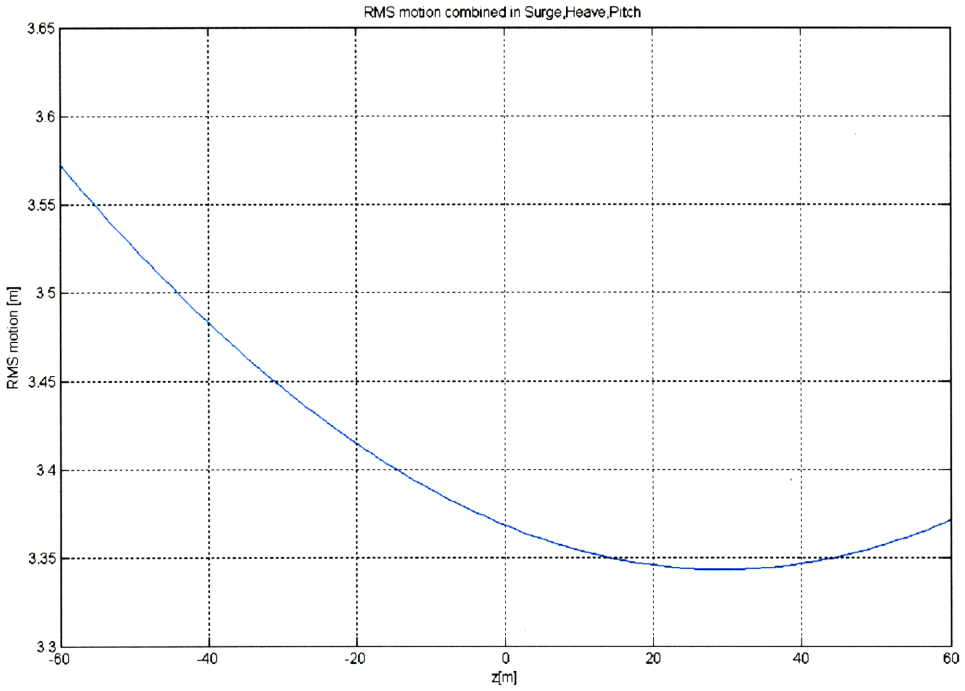

Figure15. The combined RMS motions along the z-axis of buoy.
in surge, heave, and pitch when alpha = 50 deg

As seen in the above plot, the combined motion in surge, heave, and pitch doesn't vary a lot along the buoy's vertical axis, which reveals that pitch motion is less dominant than any other modes of motion. This is the reason why the phase difference between two separate tensions at anchor couldn't be as significant as expected. Depending on which combination of design parameters such as pretensions, or fairlead positions to be applied, however, there is still a potential possibility of having those tensions being out of phase from each other.

The above plot also reveals that double-layerd catenary mooring lines will be much more effective if we can find any particular combination of design parameters such that have buoy behaves with smaller dynamic responses in heave and surge compared against pitch motions. One of the possible solutions would be a platform designed specially for a low heave exciting force, such as a semi-submersible platform, etc. A parametric design analysis is a promising solution for this as well, which is shown at the last chapter, the Pareto simulation analysis.

4.4.2. When k1 = 0.980 m/m , k2 = 0.985, T^1_{pre} =2E6 N, T^2_{pre} =1.5E6 N

4.4.2.1. Specifications

Properties		Values		
Platform	Diameter [m]		14	
	Draft [m]		60	
	Displacement [metric tons]		9485.66	
Concrete	Concrete Mass [metric tons]		8042.43	
	Concrete Height [m]		20.38	
Center of Gravity [m]			-39.68	
Center of Buoyancy [m]			-30	
Sea condition	Water depth [m]		150	
Mooring	Alpha [degree]	Varies	Minimum	Maximum
			30	75
	k1 [m/m]		0.980	
	k2 [m/m]		0.985	
	Fairlead Location, L1 [m/m]		1	
	Fairlead Location, L2 [m/m]		-0.5	
	* EA_Acr [N]		200E6	
	* EA1 [N]		100E6	
	* EA2 [N]		100E6	
	Pretension1, T^1_{pre} [N]		2E6	
	Pretension2, T^2_{pre} [N]		1.5E6	
	MBL_Acr [N]		10E6	
	MBL1 [N]		5E6	
	MBL2 [N]		5E6	

(Bottom Layer: k1,L1, Top Layer: k2,L2)

* EA = $K_{rd} \times MBL$ (E: the catenary modulus, EA: the gradient of loading, K_{rd} : the dynamic axial stiffness, MBL: the minimum breaking load of the catenary)

4.4.2.2. Dynamic Performances

The system dynamic behaviors in each RMS value have been evaluated varying the catenary angle from sea bed, and been plotted below.

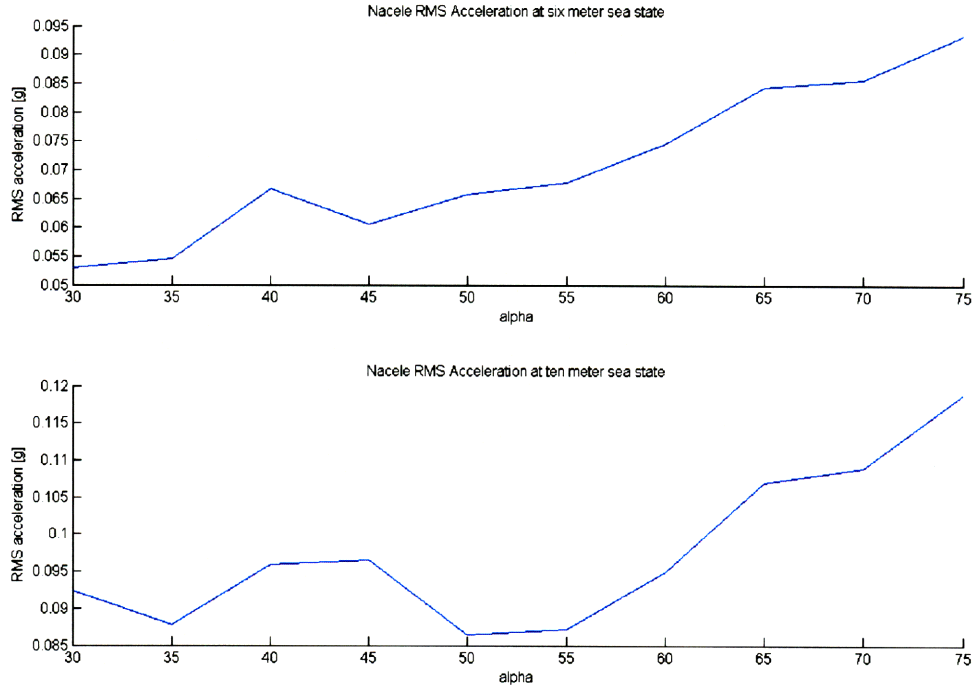

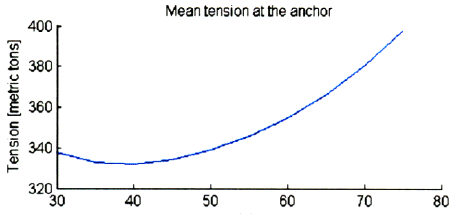
Mean tension at the anchor
Tension [metric tons]
alpha

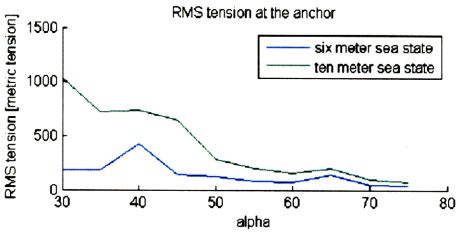
RMS tension at the anchor
RMS tension [metric tension]
six meter sea state
ten meter sea state
alpha

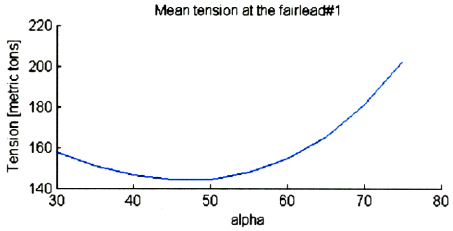
Mean tension at the fairlead#1
Tension [metric tons]
alpha

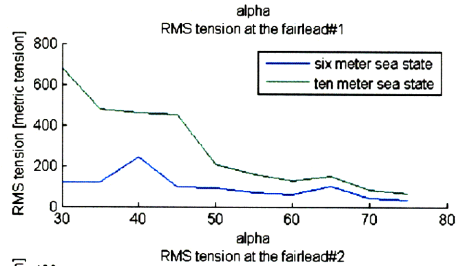
RMS tension at the fairlead#1
RMS tension [metric tension]
six meter sea state
ten meter sea state
alpha

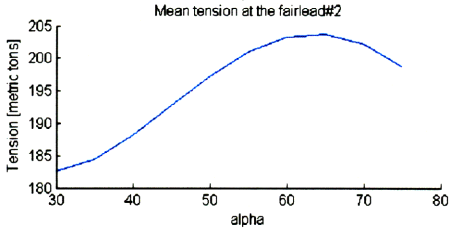
Mean tension at the fairlead#2
Tension [metric tons]
alpha

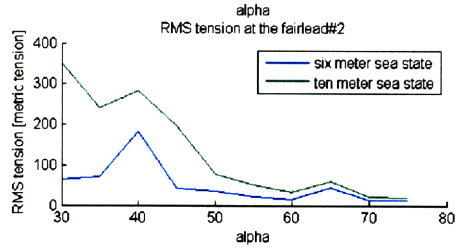
RMS tension at the fairlead#2
RMS tension [metric tension]
six meter sea state
ten meter sea state
alpha

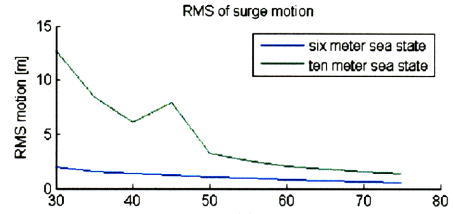
RMS of surge motion
RMS motion [m]
six meter sea state
ten meter sea state
alpha

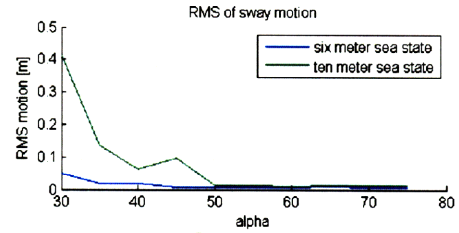
RMS of sway motion
RMS motion [m]
six meter sea state
ten meter sea state
alpha

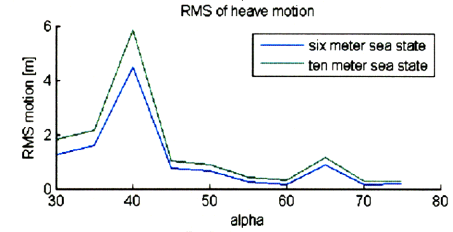
RMS of heave motion
RMS motion [m]
six meter sea state
ten meter sea state
alpha

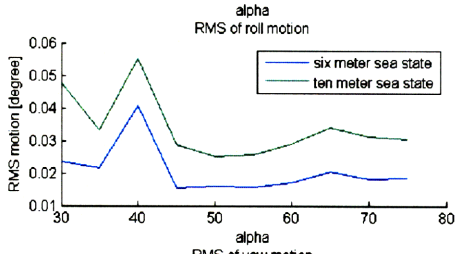
RMS of roll motion
RMS motion [degree]
six meter sea state
ten meter sea state
alpha

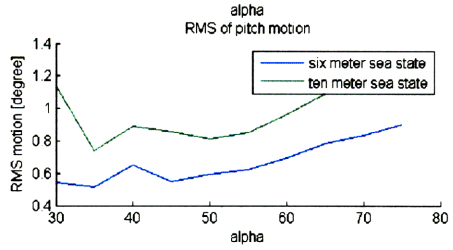
RMS of pitch motion
RMS motion [degree]
six meter sea state
ten meter sea state
alpha

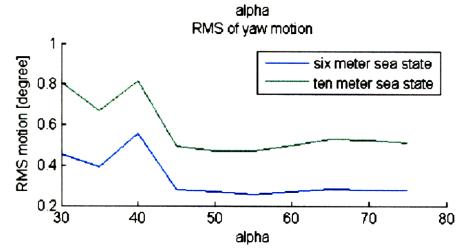
RMS of yaw motion
RMS motion [degree]
six meter sea state
ten meter sea state
alpha

The RAO for three different angles have been evaluated and compared as shown below.

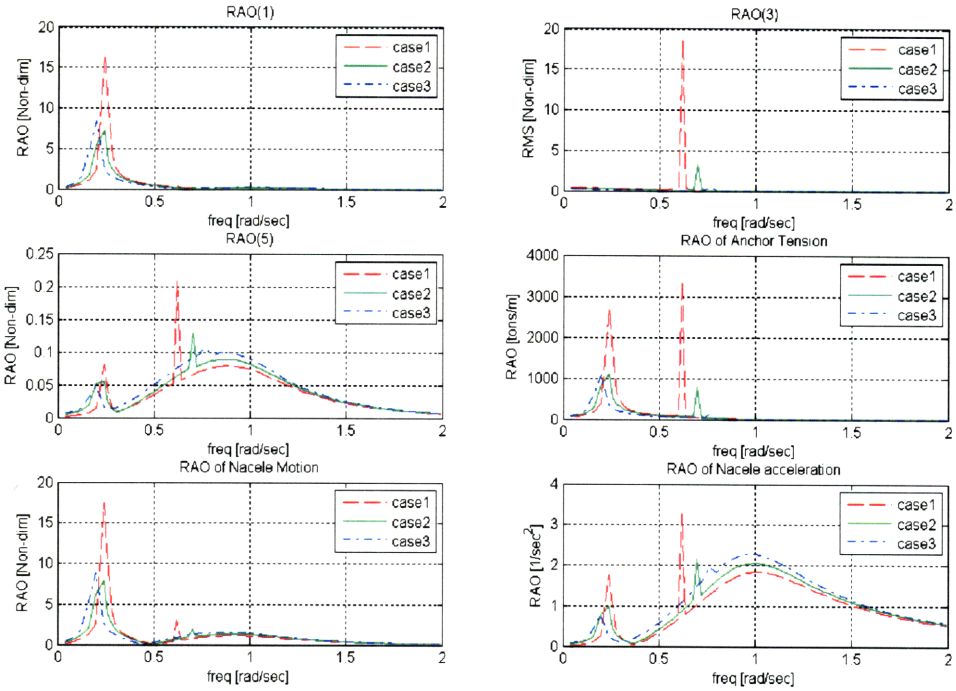

(Case1: Alpha=40; Case2: Alpha=50; Case3: Alpha=60)

4.5. BDLC (Ballasted Double-Layered Catenary)

4.5.1. When k1 = 0.980 m/m, k2 = 0.985, T^1_{pre} =2E6 N, T^2_{pre} =1.5E6 N

4.5.1.1. Specifications

Properties		Values		
Platform	Diameter [m]		14	
	Draft [m]		60	
	Displacement [metric tons]		9485.66	
Concrete	Concrete Mass [metric tons]		8042.43	
	Concrete Height [m]		20.38	
Center of Gravity [m]			-39.68	
Center of Buoyancy [m]			-30	
Sea condition	Water depth [m]		150	
Mooring	Alpha [degree]	Varies	Minimum	Maximum
			30	75
	k1 [m/m]		0.980	
	k2 [m/m]		0.985	
	Fairlead Location, L1 [m/m]		1	
	Fairlead Location, L2 [m/m]		-0.5	
	* EA_Acr [N]		200E6	
	* EA1 [N]		100E6	
	* EA2 [N]		100E6	
	Pretension1, T^1_{pre} [N]		2E6	
	Pretension,2 T^2_{pre} [N]		1.5E6	
	MBL_Acr [N]		10E6	
	MBL1 [N]		5E6	
	MBL2 [N]		5E6	
	Concrete Ballast Mass per line [metric tons]		50	

(Bottom Layer: k1,L1, Top Layer: k2,L2)

**Note: the corresponding effects on system displacement due to the concrete ballast mass is ignored during the present analysis

4.5.1.2. Dynamic Performances

The system dynamic behaviors in each RMS value have been evaluated varying the catenary angle from sea bed, and been plotted below.

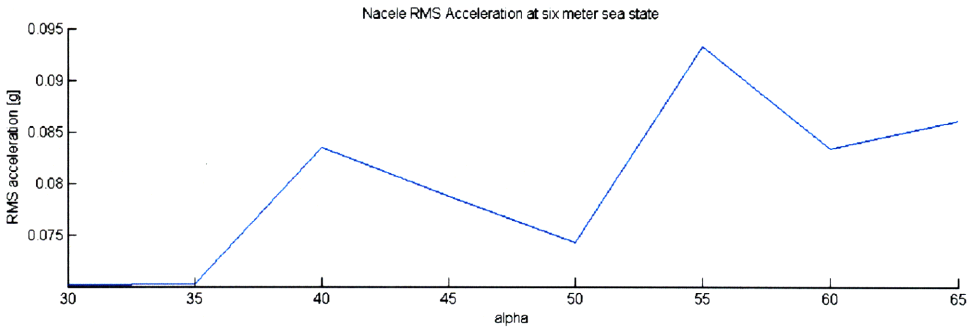

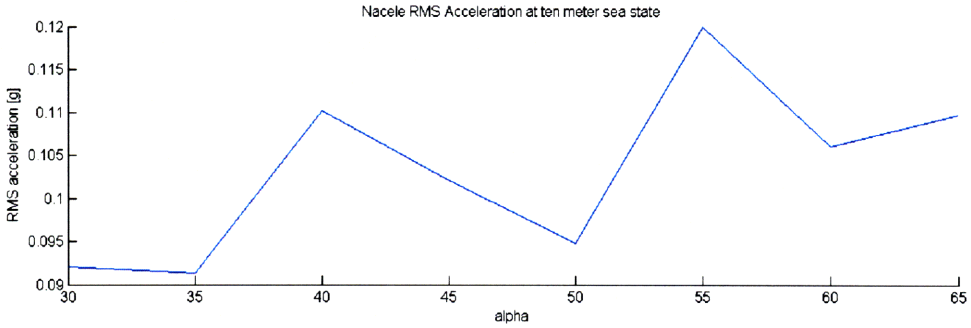

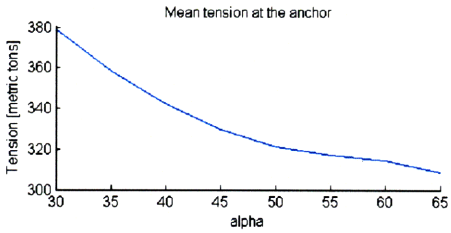
Mean tension at the anchor
Tension [metric tons]
alpha

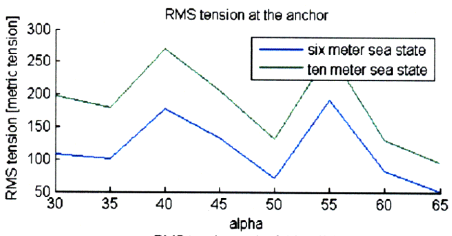
RMS tension at the anchor
RMS tension [metric tension]
six meter sea state
ten meter sea state
alpha

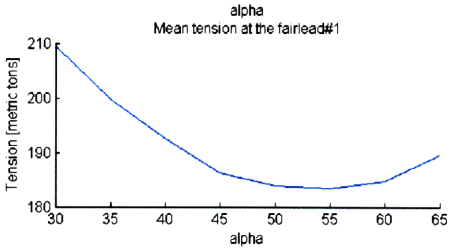
Mean tension at the fairlead#1
Tension [metric tons]
alpha

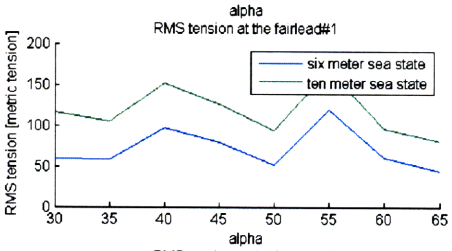
RMS tension at the fairlead#1
RMS tension [metric tension]
six meter sea state
ten meter sea state
alpha

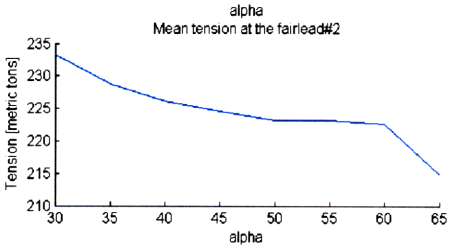
Mean tension at the fairlead#2
Tension [metric tons]
alpha

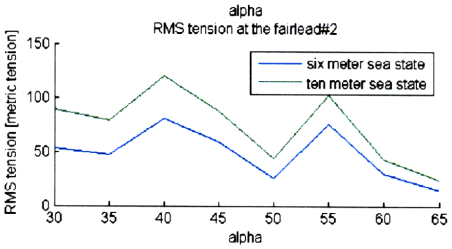
RMS tension at the fairlead#2
RMS tension [metric tension]
six meter sea state
ten meter sea state
alpha

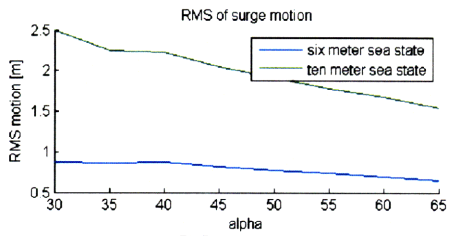
RMS of surge motion
RMS motion [m]
six meter sea state
ten meter sea state
alpha

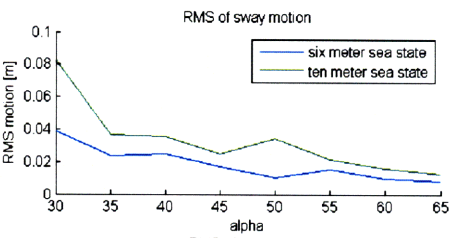
RMS of sway motion
RMS motion [m]
six meter sea state
ten meter sea state
alpha

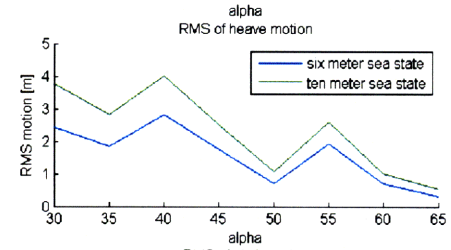
RMS of heave motion
RMS motion [m]
six meter sea state
ten meter sea state
alpha

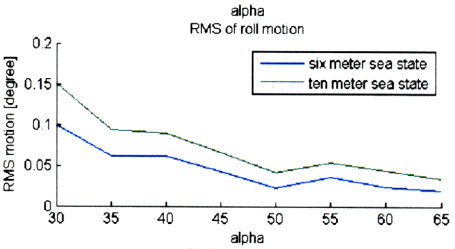
RMS of roll motion
RMS motion [degree]
six meter sea state
ten meter sea state
alpha

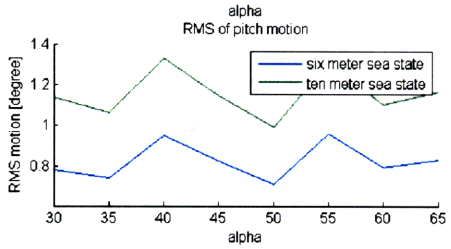
RMS of pitch motion
RMS motion [degree]
six meter sea state
ten meter sea state
alpha

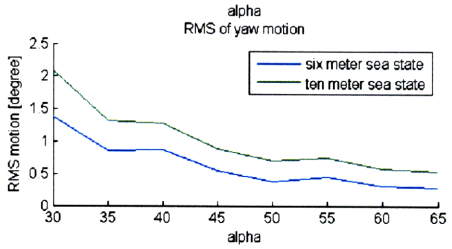
RMS of yaw motion
RMS motion [degree]
six meter sea state
ten meter sea state
alpha

The RAO for three different angles have been evaluated and compared as shown below.

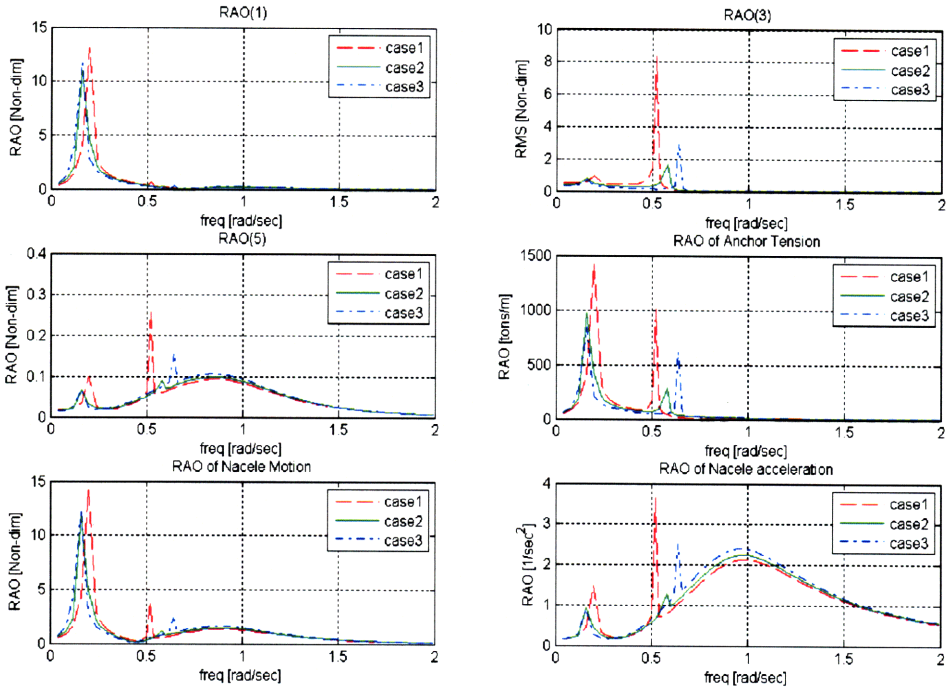

(Case1: Alpha=40; Case2: Alpha=50; Case3: Alpha=60)

4.6. Comparison of DLC and BDLC

4.6.1. When Alpha = 50 deg, k1 = 0.980 m/m, k2 = 0.985 m/m, T^1_{pre} =2E6 N, T^2_{pre} =1.5E6 N

4.6.1.1. SLC

Sea States, Hs		6m	10m	Units
RMS Nacelle Acceleration		0.066	0.086	g
RMS Motions	Surge	1.050	3.255	m
	Heave	0.638	0.869	m
	Pitch	0.594	0.809	degree
*Fairlead #1 Tension	Mean	144.392	144.392	metric tons
	RMS	90.207	206.018	metric tons
Fairlead #2 Tension	Mean	197.316	197.316	metric tons
	RMS	34.876	78.139	metric tons
Anchor #1 Tension	Mean	143.475	143.475	metric tons
	RMS	90.207	206.018	metric tons
Anchor #2 Tension	Mean	195.480	195.480	metric tons
	RMS	34.366	77.733	metric tons
Anchor Tension Combined	Mean	338.955	338.955	metric tons
	RMS	118.948	279.290	metric tons

(*All of the tension components are picked up from windward side) get_data.m zzzztotal

Table22. DLC with k1=0.980, k2=0.985

4.6.1.2. BSLC with suspension ballast of 50 metric tons

Sea States, Hs		6m	10m	Units
RMS Nacelle Acceleration		0.074	0.095	g
RMS Motions	Surge	0.777	1.911	m
	Heave	0.698	1.076	m
	Pitch	0.709	0.991	degree
*Fairlead #1 Tension	Mean	183.957	183.957	metric tons
	RMS	51.311	93.516	metric tons
Fairlead #2 Tension	Mean	223.217	223.217	metric tons
	RMS	25.927	43.761	metric tons
Anchor #1 Tension	Mean	144.902	144.902	metric tons
	RMS	51.887	94.269	metric tons
Anchor #2 Tension	Mean	176.514	176.514	metric tons
	RMS	25.927	43.761	metric tons
Anchor Tension Combined	Mean	321.416	321.416	metric tons
	RMS	72.225	131.670	metric tons

(*All of the tension components are picked up from windward side) get_data.m zzzztotal

Table23. BDLC with k1=0.980, k2=0.985

As seen in the above table, smaller RMS tensions have been achieved by a ballasted catenary in the case of DLC as well. The effective tension acting on the anchor also decreases significantly especially at the ten meter sea state. Another issue which should be stated about DLC, is that the complexity of DLC configuration makes the Pareto analysis simulation more desired and recommended. It might be inefficient for this catenary system to be studied and stated well in an analytical manner.

4.7. SLC with vertical viscous damping plates

The floating platform of the present system is a spar buoy that is a lightly damped system in surge, and also has a smaller exciting force at the long wave region. Therefore, an additional viscous damping effect will have a significant impact on the surge RAO peak at its resonant frequency, and drives the motion response down. At this chapter, the viscous effect due to vertical plates installed along the buoy is being studied. The viscous effect due to spar buoy itself and mooring lines have not been taken into account in this analysis, and therefore any possible vortex induced vibration (VIV) has been neglected.

In this particular design, the effect of heave motion on the RMS tensions is insignificant primarily because the heave resonant frequency isn't located near the sea spectrum peak, and therefore it's impact on the tension RAO doesn't affect the entire RMS. This is why the horizontal damping plates are not considered in this chapter.

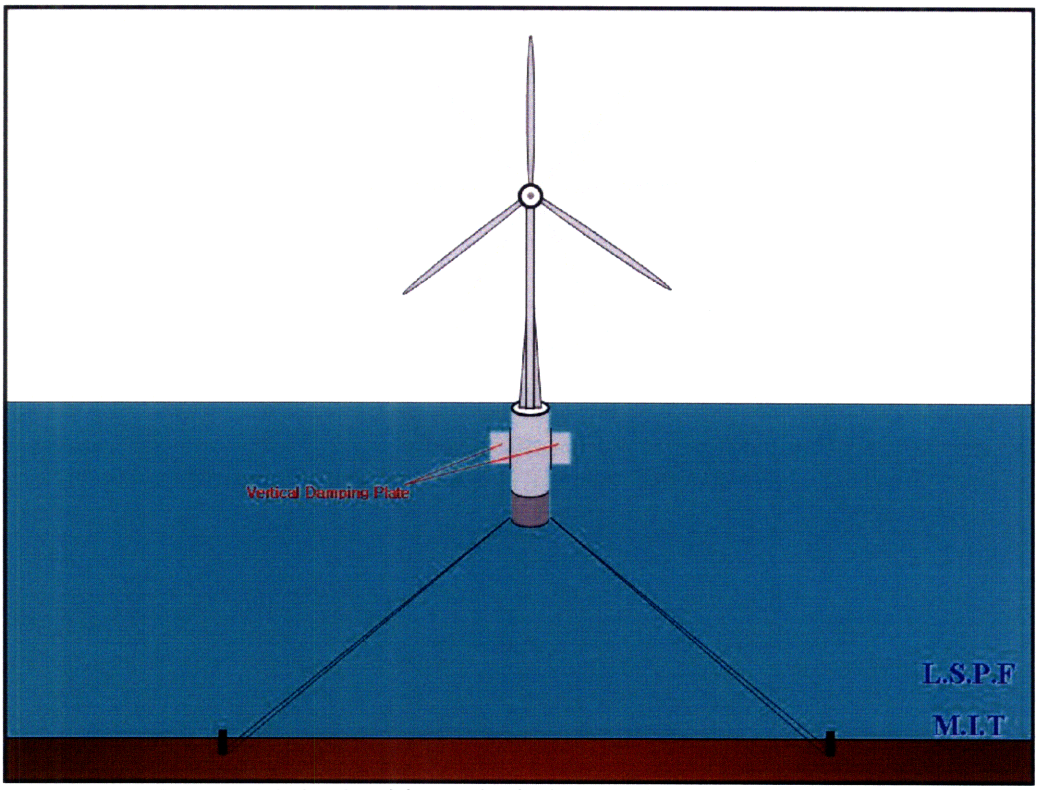

Fugure16. SLC with vertical viscous damping plates

4.7.1. Equivalent Linearization Method

The surge equation can be written as below.

$$(M + A_{11})\ddot{\xi}_1 + B_{11}\dot{\xi} + B_v\dot{\xi}|\dot{\xi}| + C_{11}\xi = X_1$$

In order to apply the frequency domain analysis based on the linear wave induced motion theory, all components in the equation of motion have to be in a linear form. The viscous damping force is in quadratic function of velocity. This nonlinear damping term can be linearized by a method of equivalent linearization technique as shown below.

$$B_v\dot{\xi}_1|\dot{\xi}_1| = B_e\dot{\xi}_1$$

$$\begin{pmatrix} B_e = 2\left(\frac{2}{\pi}\right)^{1/2} \cdot B_v \cdot \sigma_{\dot{\xi}_1} \\ B_v = \frac{1}{2}\rho \cdot S \cdot C_D \\ KC = 2\pi\frac{a}{D} \end{pmatrix}$$

Where, B_e =equivalent linear viscous damping coefficient

B_v =viscous damping coefficient

S =frontal surface area of the damping plate

C_D =damping coefficient

KC =Keulegan-Carpenter (KC) number

a =amplitude of surge oscillation

D =Diameter of the damping plate

4.7.2. Comparison of SLC with or without damping plates

The RSM values for nacelle acceleration and tensions have been compared at the 10 meter sea state, and tabulated below.

4.7.2.1. When Alpha = 50 deg, k = 0.990 m/m, T_{pre} =2E6 N

Sea States, Hs		10m	Units
RMS Nacelle Acceleration		0.167	g
RMS Motions	Surge	6.150	m
	Heave	0.401	m
	Pitch	3.286	degree
*Fairlead Tension	Mean	275.120	metric tons
	RMS	389.949	metric tons
*Anchor Tension	Mean	274.917	metric tons
	RMS	389.949	metric tons

(*All of the tension components are picked up from windward side)

Table24. SLC without damping plate

Sea States, Hs		10m	Units
RMS Nacelle Acceleration		0.146	g
RMS Motions	Surge	4.969	m
	Heave	0.398	m
	Pitch	2.555	degree
*Fairlead Tension	Mean	275.120	metric tons
	RMS	332.300	metric tons
*Anchor Tension	Mean	274.917	metric tons
	RMS	332.300	metric tons

(*All of the tension components are picked up from windward side)

Table25. SLC with damping plate

Due to the damping effect by vertical damping plates, the RMS tension has been decreased by 60 tons, the nacelle acceleration has been decreased down by 0.02g, and the surge RMS motion has been decreased down by 1m. The effect on RMS tension is

actually huge, and the reason for that is explained in detail at the RAO plots shown below.

RAO Comparison

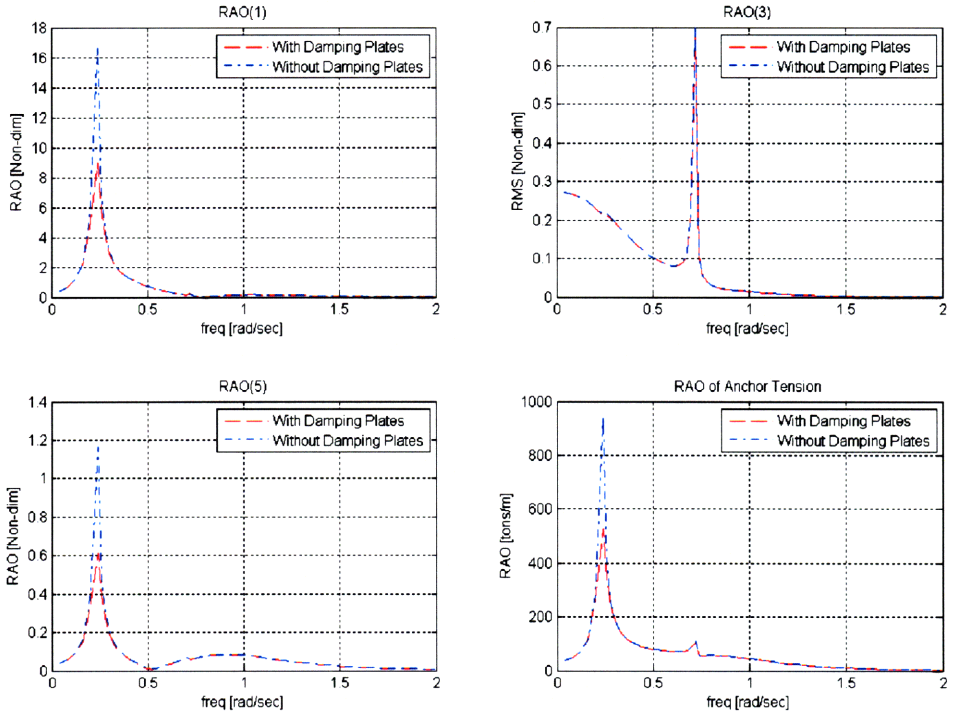

Figure17. Comparison between with or without damping plates (SLC, k=0.990, alpha=50deg)

For the SLC with k of 0.990 m/m and alpha of 50 deg, the four RAOs in surge, heave, pitch, and anchor tension have been compared and plotted as shown above. As seen in the plots above, the viscous damping effect from the vertical damping plates is so significant. The peaks of RAO in surge and pitch decrease by more than 50 percent due to the damping in surge mode of motion. The first peak of the RAO in tension at anchor also decreases by 50 percent as well. The spectral density function for six and ten meter sea state is mostly located in the range of 0.2 ~ 0.4 rad/sec. The first peak of the tension RAO is located right at this region, and this is the reason why its effect on RMS tension is so significant as well.

However, the viscous flow effect from damping plates on RMS values definitely depend on the resonant frequency in surge, and the mean period of a specific sea state's spectral density function we are interested in. In other words, despite of the large drop of surge RAO peak at its resonant frequency, it may not be able to affect the entire RMS values unless it is located near the sea spectrum peak. Of course, the resonant frequency in surge motion depends on all other design parameters such as the mooring system configuration, EA, or location of fairlead, etc.

5. Pareto optimization analysis and simulations

All designs for spar buoy floating wind turbine with all possible combinations of design parameters are studied in this chapter. In order to find any particular group of design parameters that leads the entire system to the best dynamic performance condition, a parametric design process has been applied having four variables; the pretension on mooring line, the catenary angle at anchor, EA, and the location of fairlead in addition to the type of mooring system (SLC, DLC). The BSLC and BDLC have not been included in this chapter. The fairlead location varies from -0.5 to 1.0 m/m, but it becomes fixed as 1.0 m/m if the alpha is designed to be larger than 50 deg.

Every design presented in this chapter fully satisfies all of the design constraints defined at chapter 3.6. The plots for Pareto front are also being presented at each set. There are two types of sea state being used which are; 10 m and 6 m significant wave height respectively, and two types of water depths which are; 150m and 300m respectively.

5.1. Water depth = 150m

5.1.1. SLC

5.1.1.1. All Designs

5.1.1.1.1. 10m Sea State

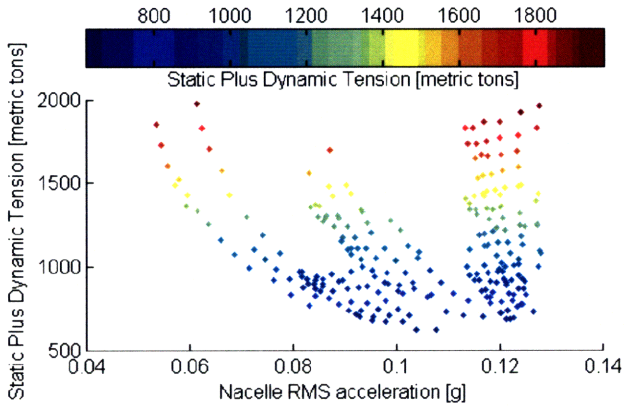

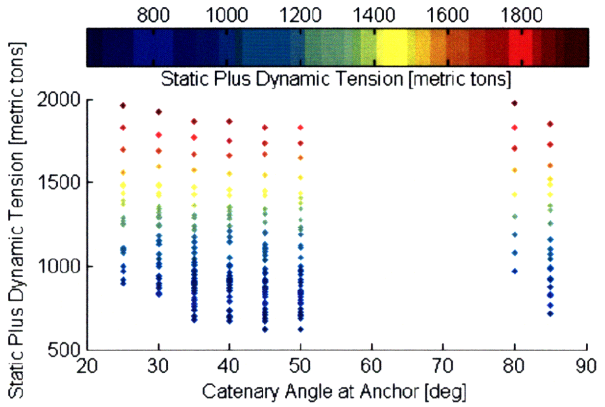

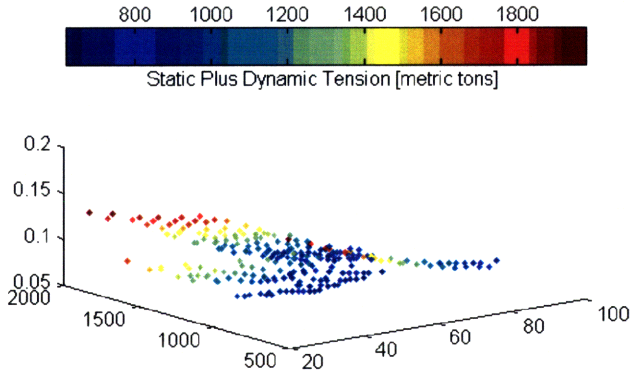

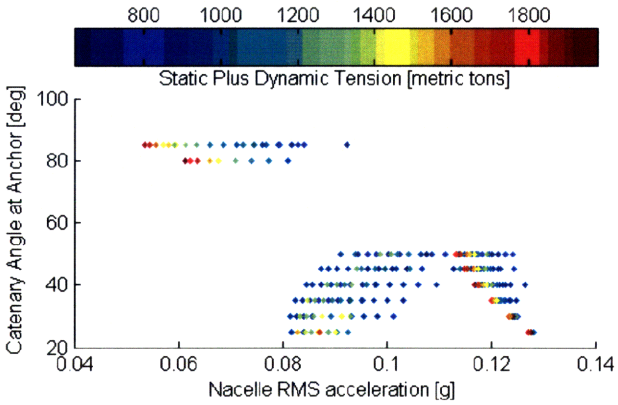

5.1.1.1.2.6m Sea State

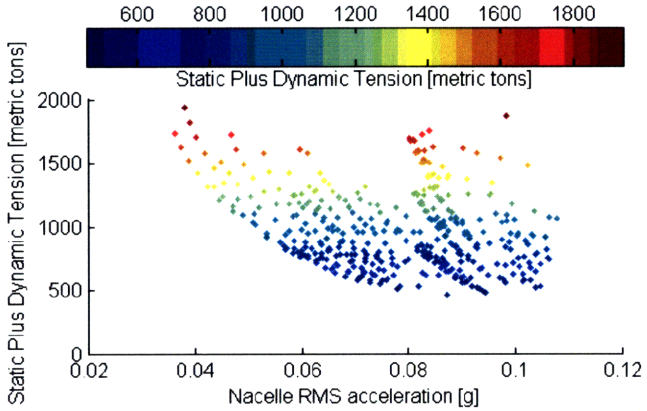

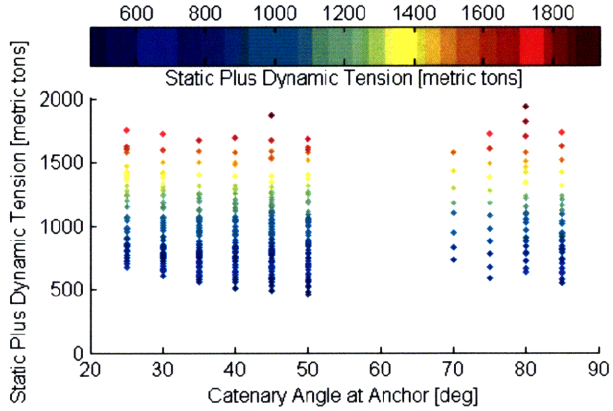

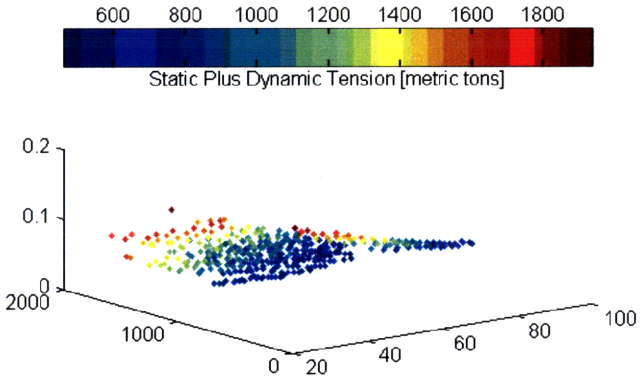

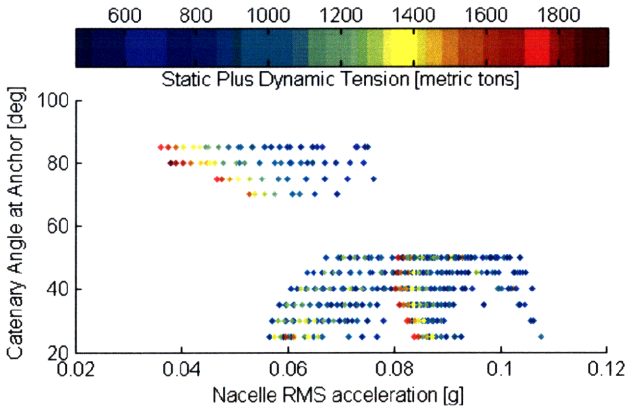

5.1.1.2. Pareto Fronts

5.1.1.2.1. 10m Sea State

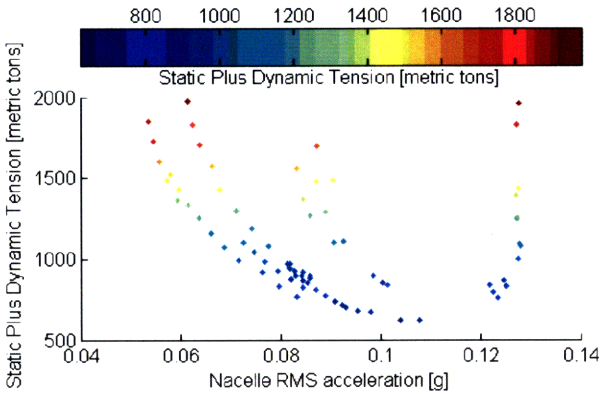

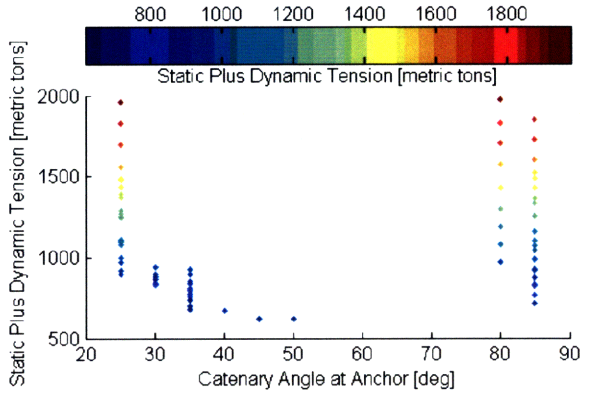

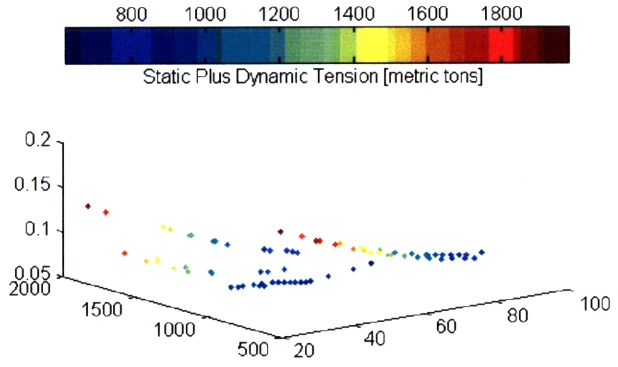

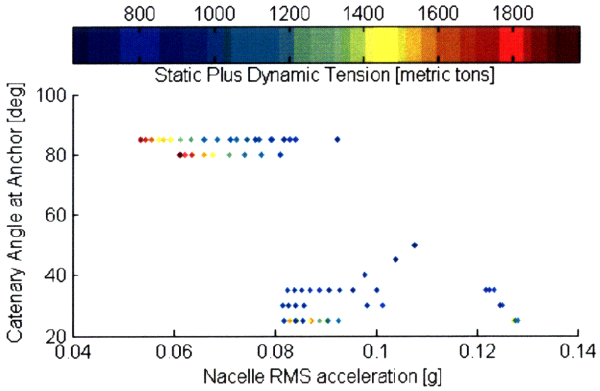

5.1.1.2.2.6m Sea State

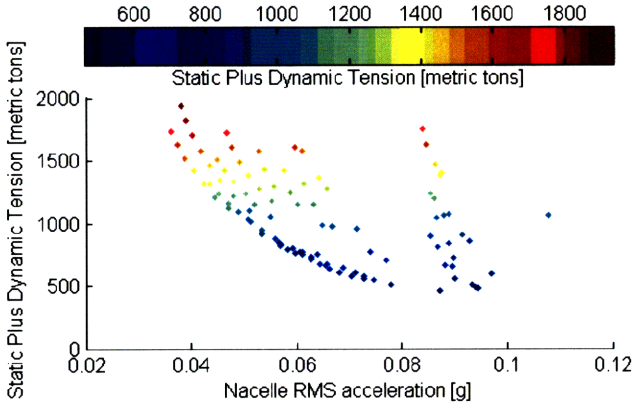

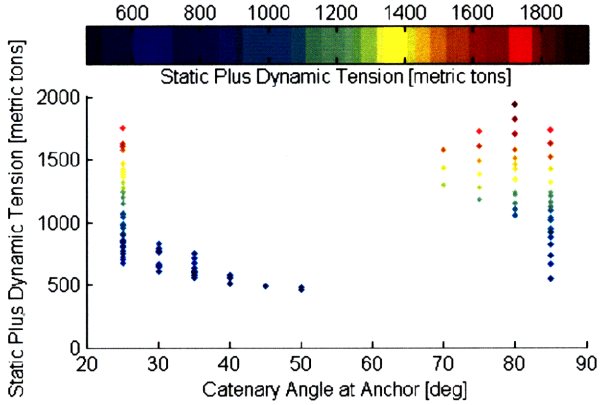

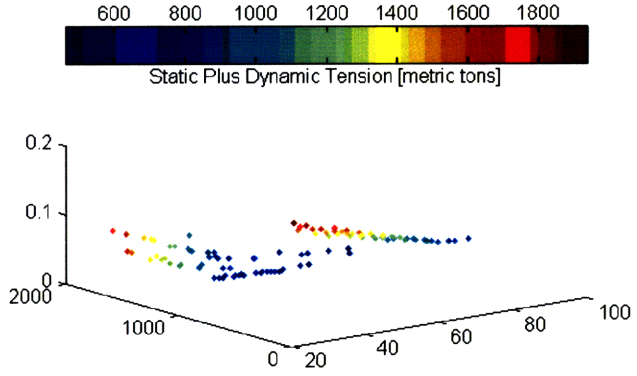

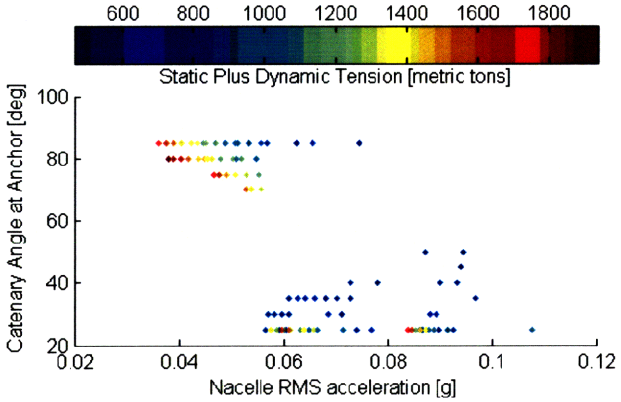

5.1.2. DLC

5.1.2.1. All Designs

5.1.2.1.1. 10m Sea State

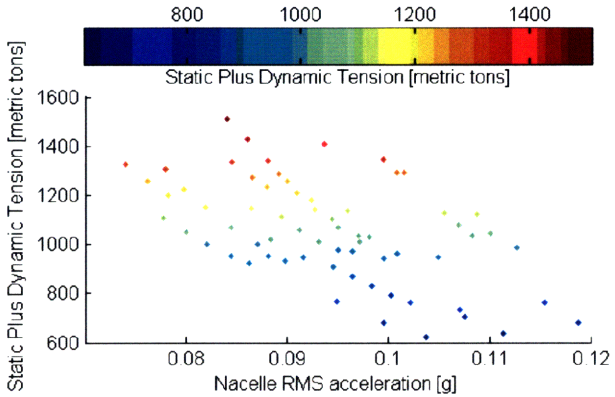

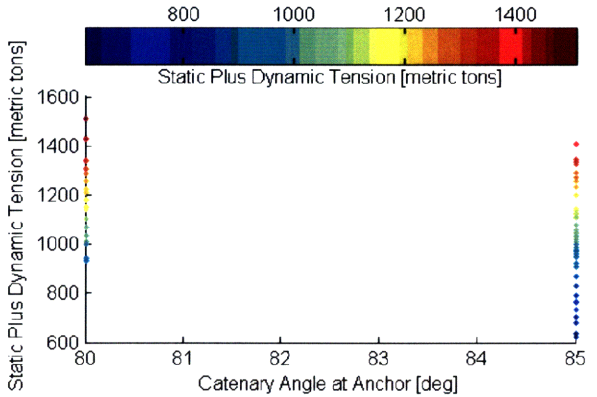

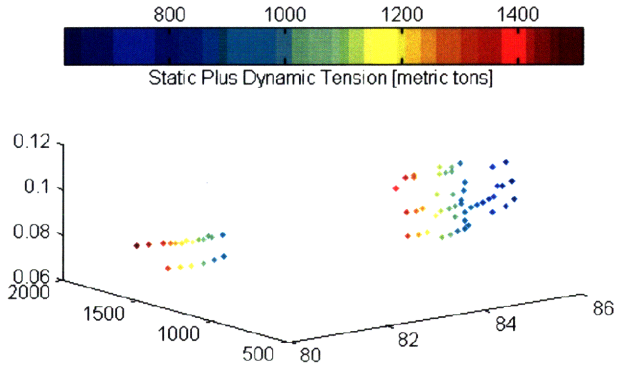

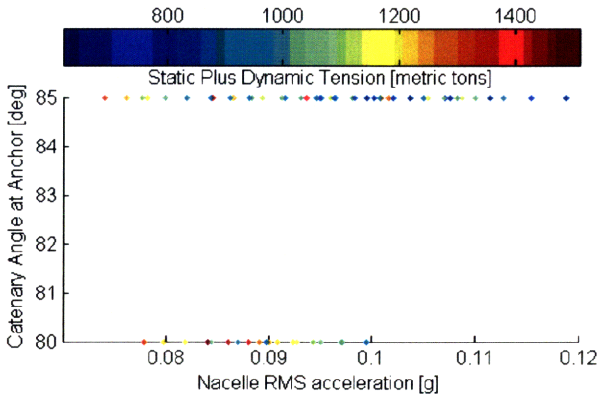

5.1.2.1.2.6m Sea State

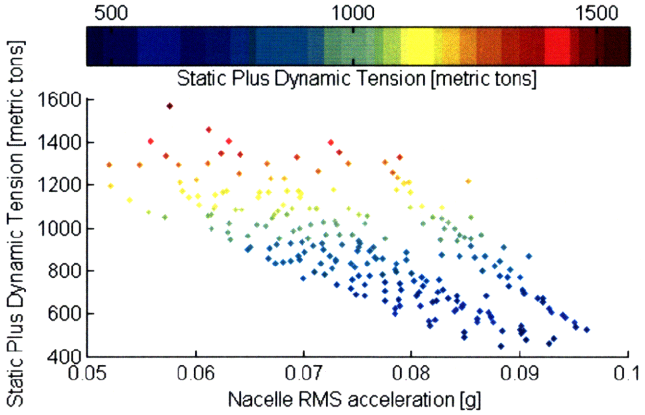

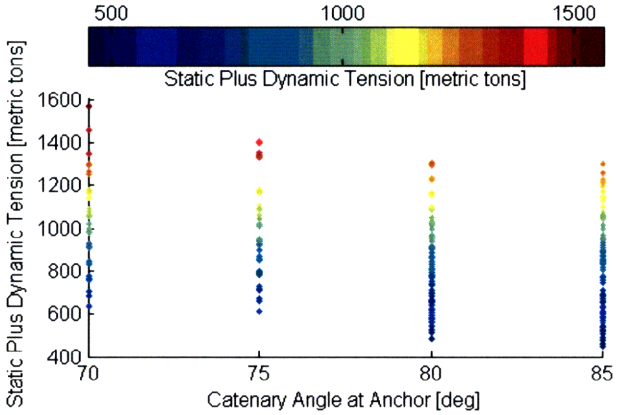

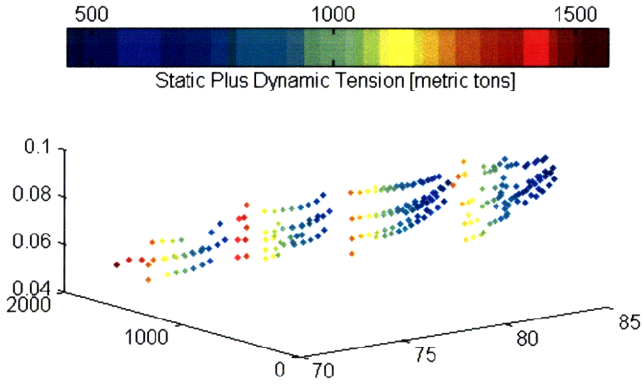

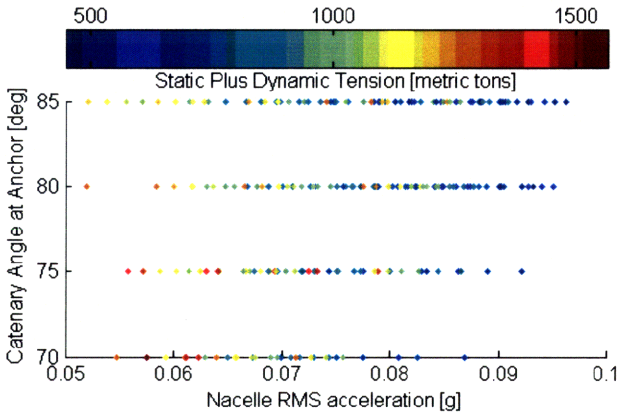

5.1.2.2. Pareto Fronts

5.1.2.2.1. 10m Sea State

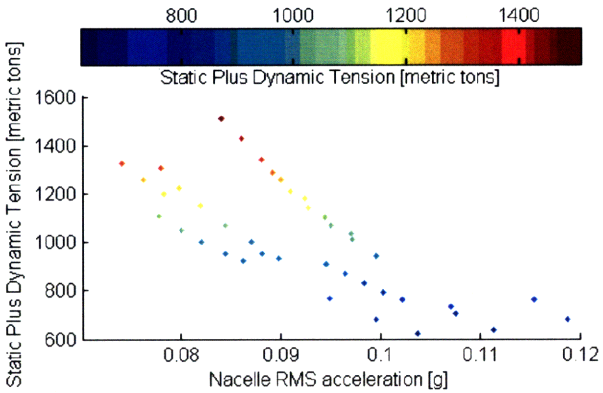

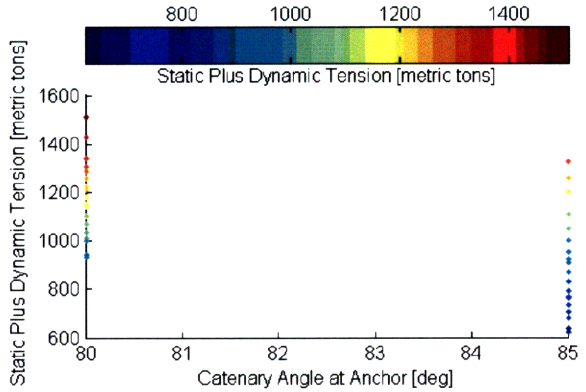

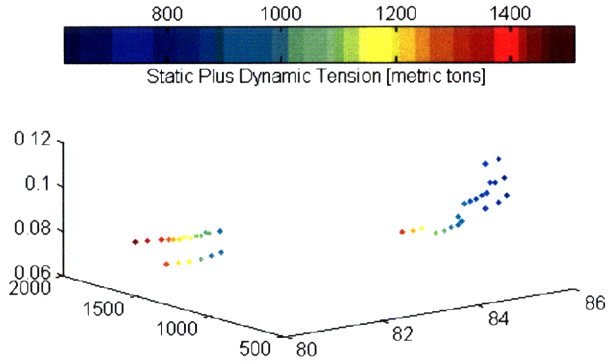

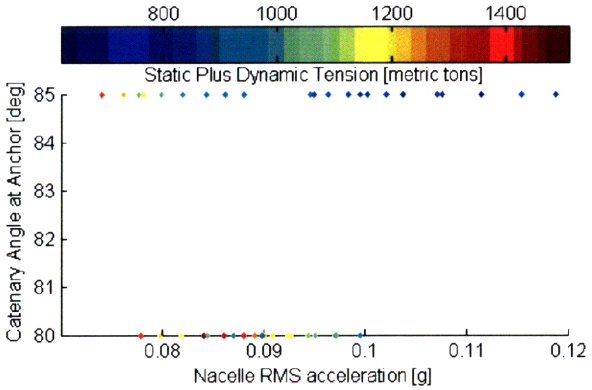

5.1.2.2.2.6m Sea State

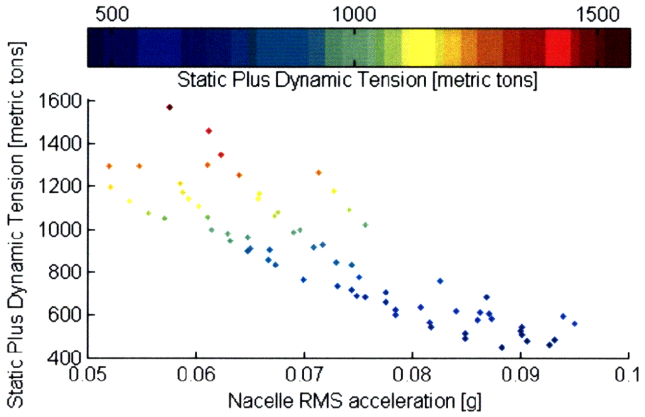

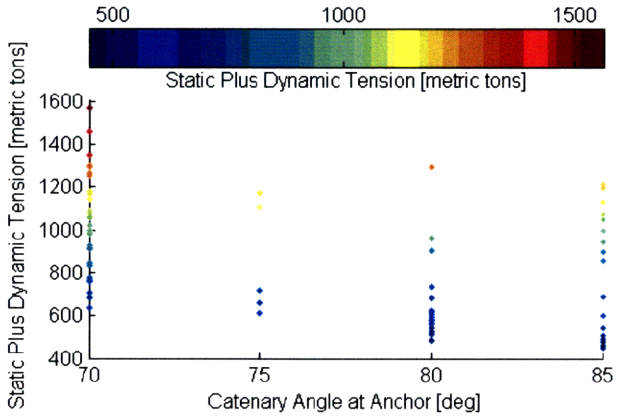

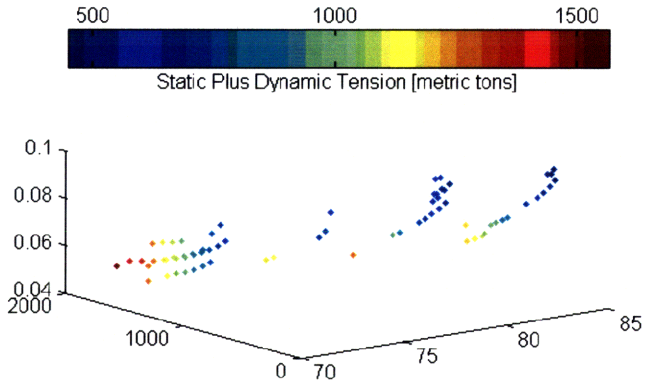

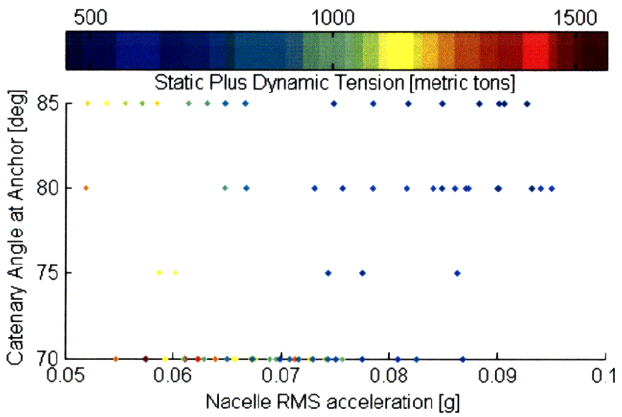

5.2. Water depth = 300m

5.2.1. SLC

5.2.1.1. All Designs

5.2.1.1.1 10m Sea State

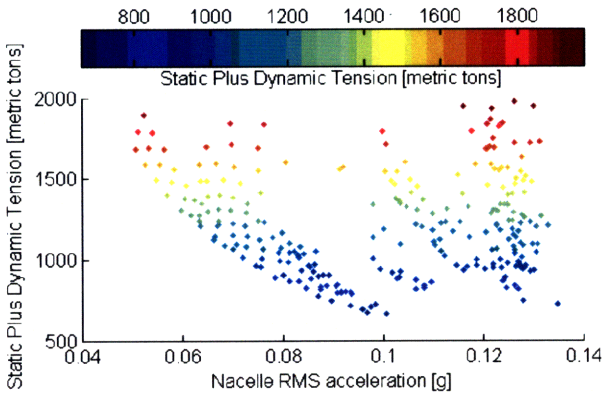

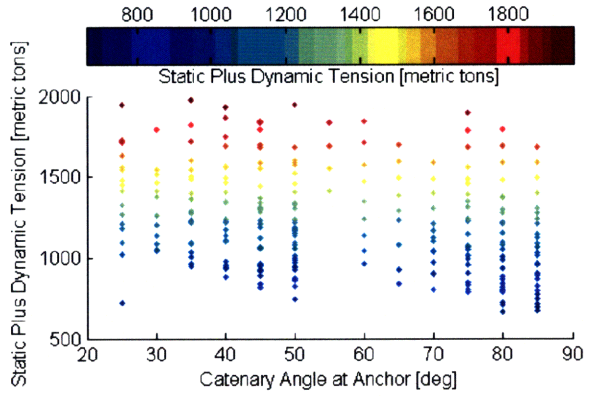

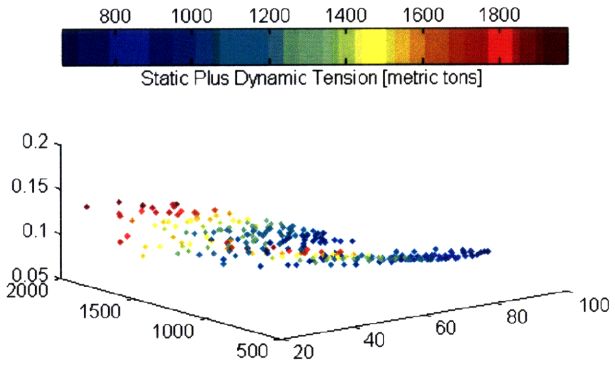

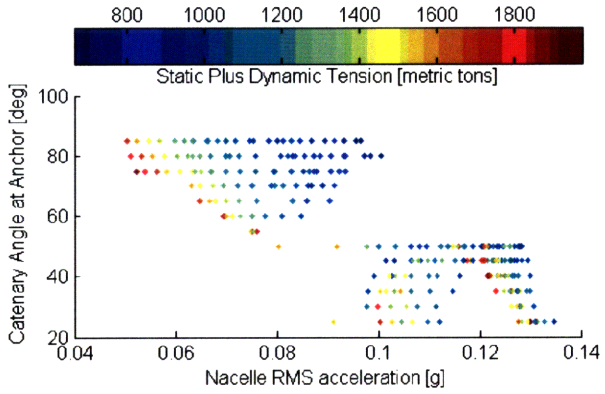

5.2.1.1.2.6m Sea State

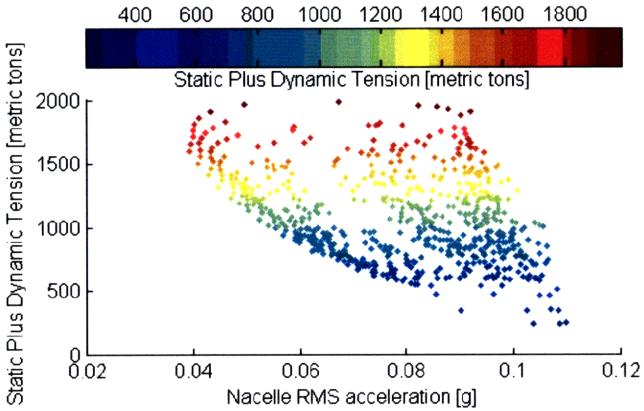

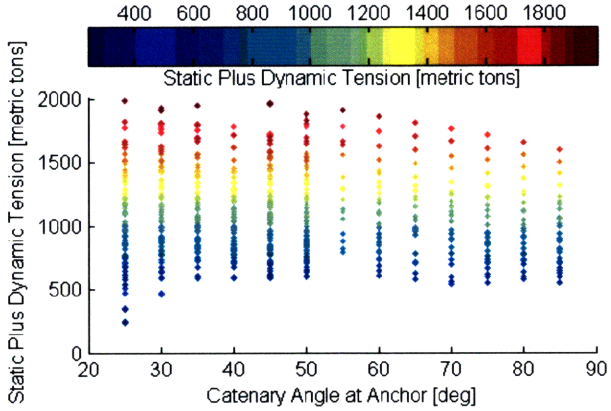

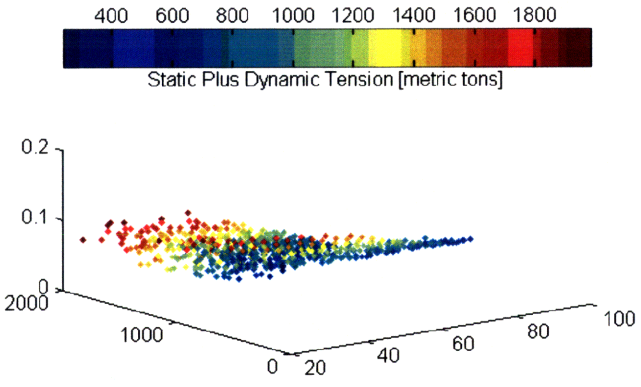

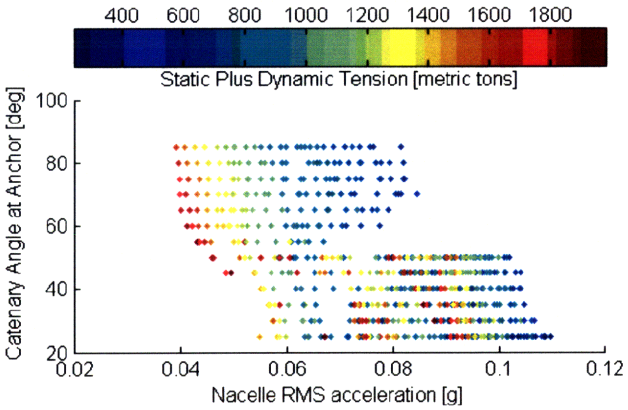

5.2.1.2. Pareto Fronts

5.2.1.2.1. 10m Sea State

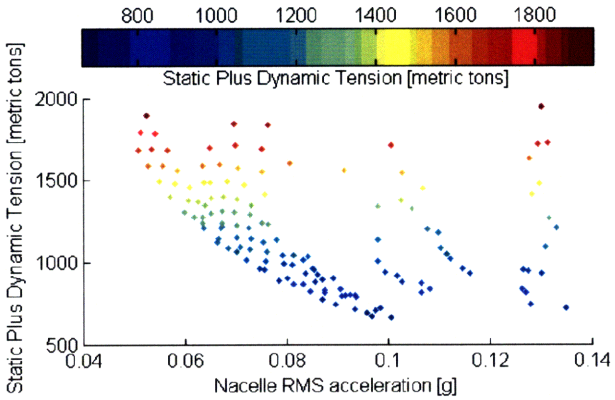

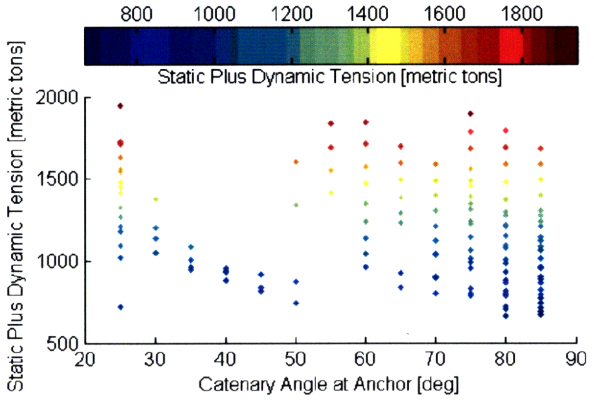

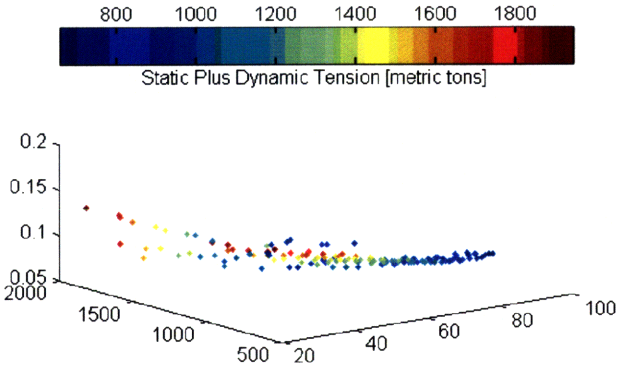

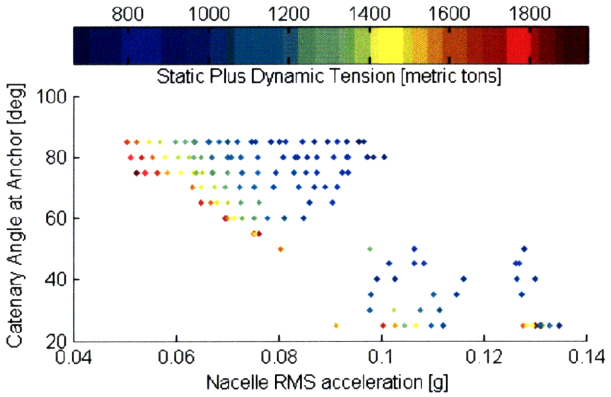

5.2.1.2.2.6m Sea State

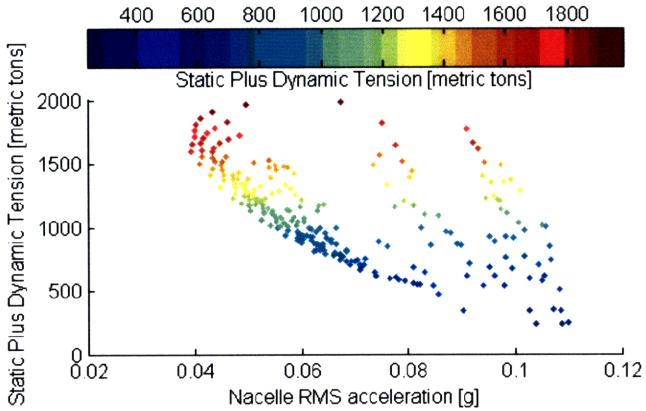

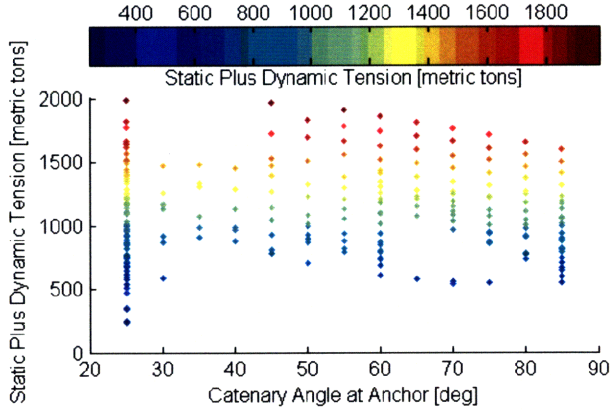

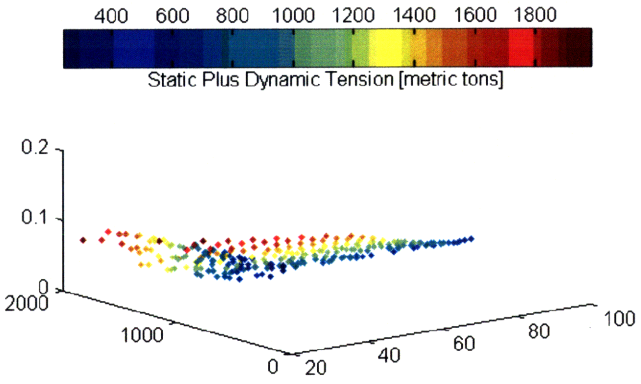

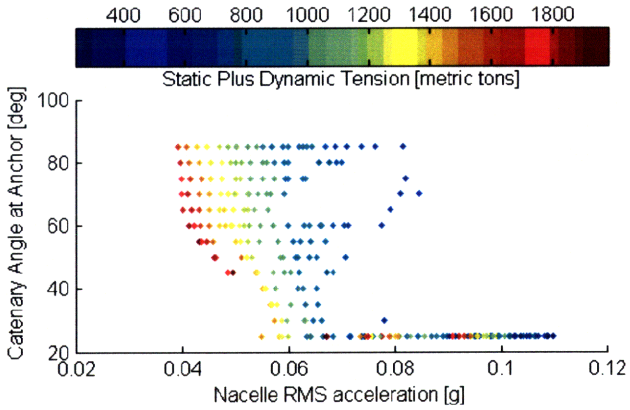

5.2.2. DLC

5.2.2.1. All Designs

5.2.2.1.1. 10m Sea State

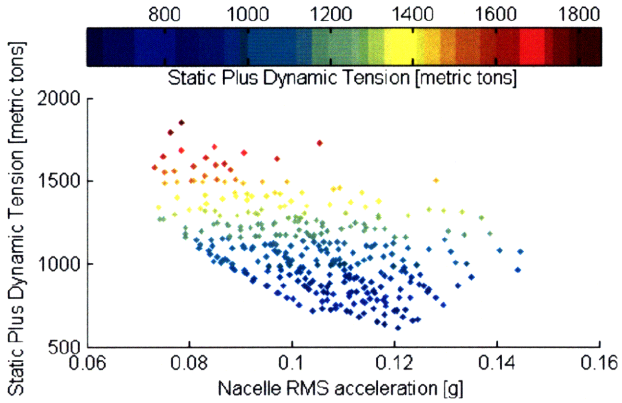

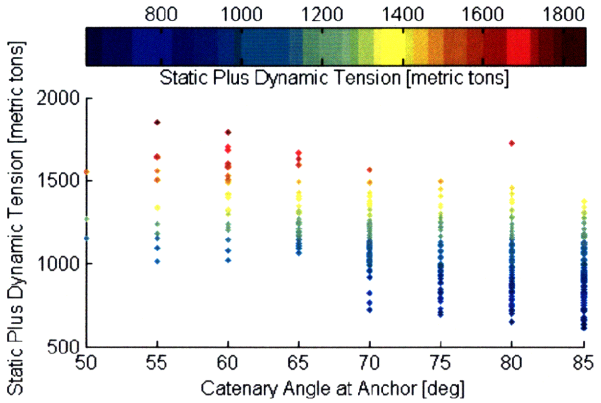

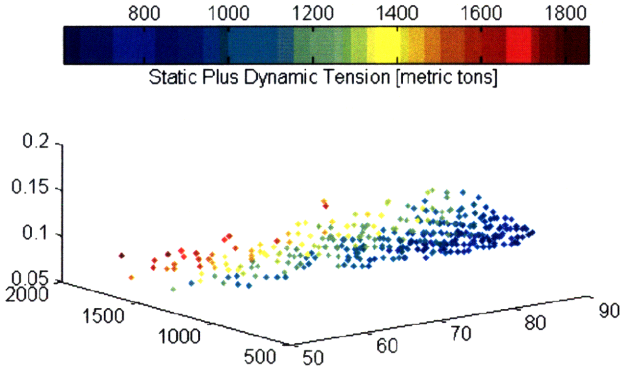

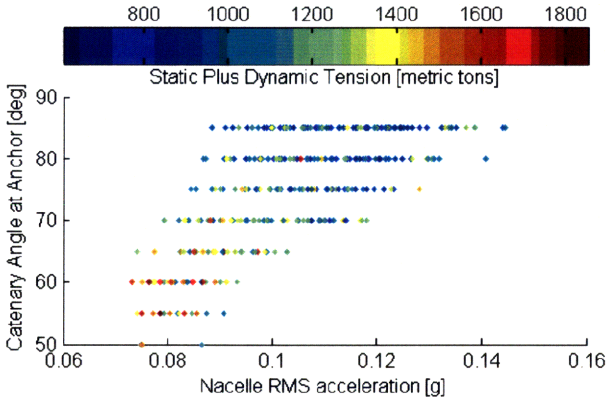

5.2.2.1.2.6m Sea State

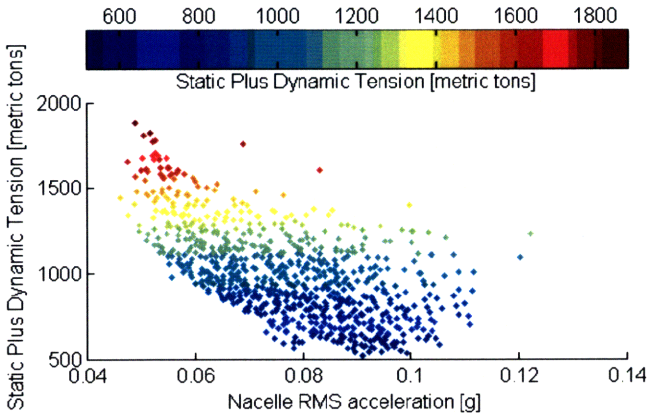

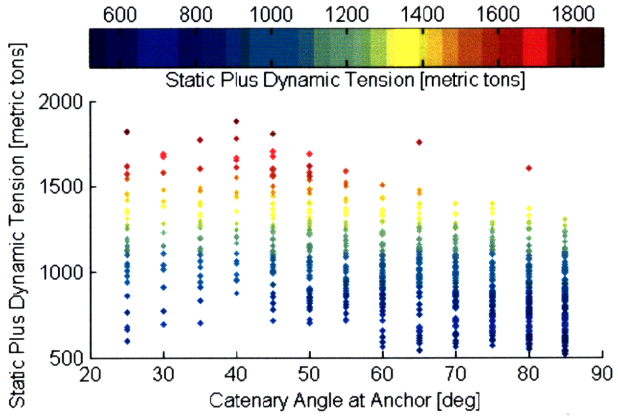

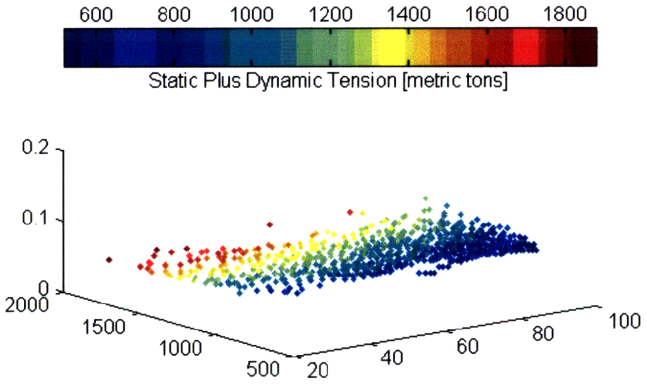

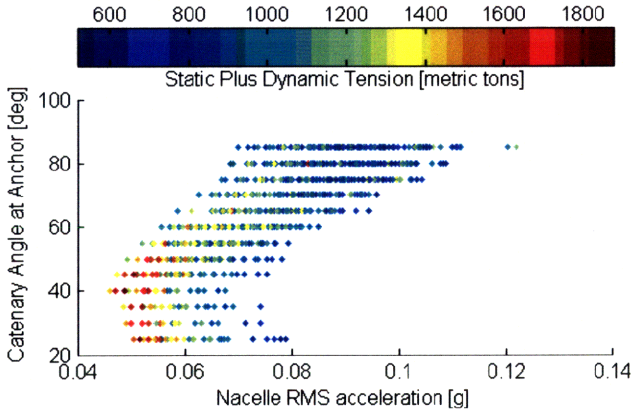

5.2.2.2. Pareto Fronts

5.2.2.2.1. 10m Sea State

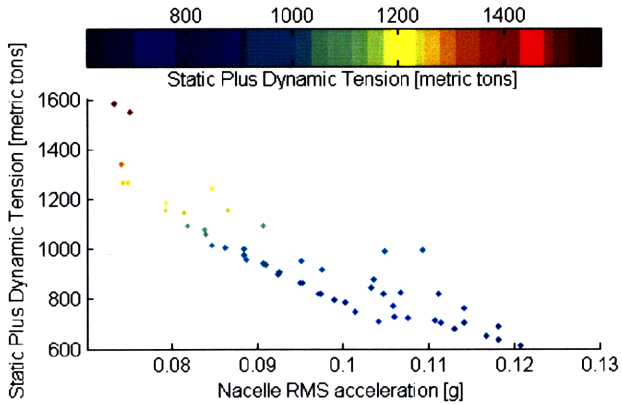

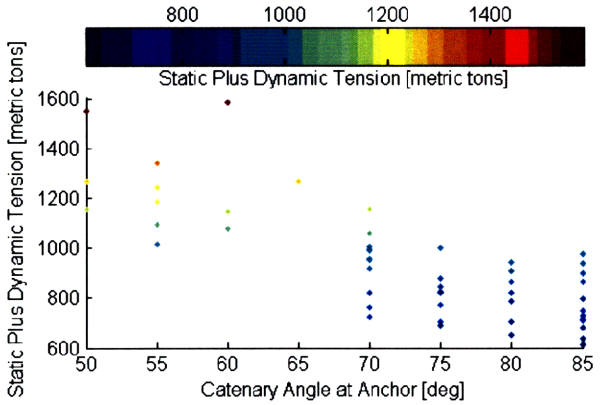

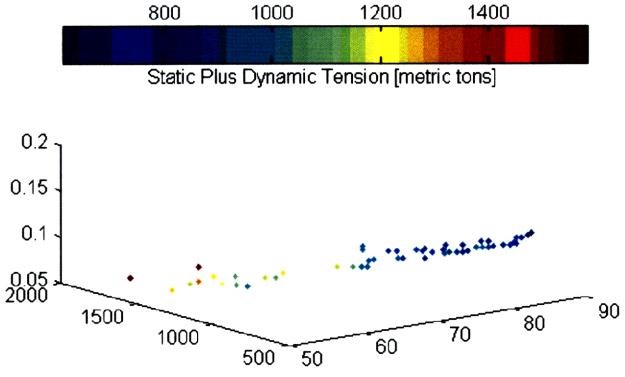

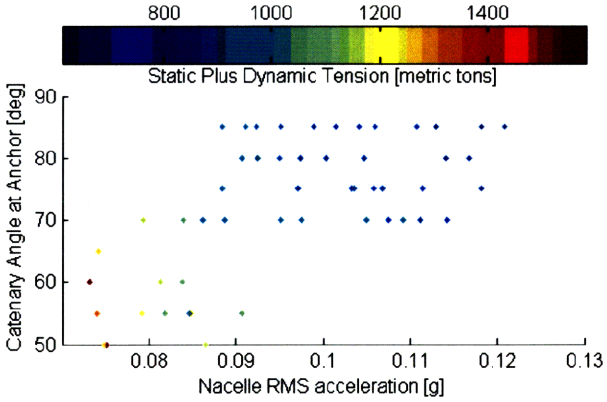

5.2.2.2.2.6m Sea State

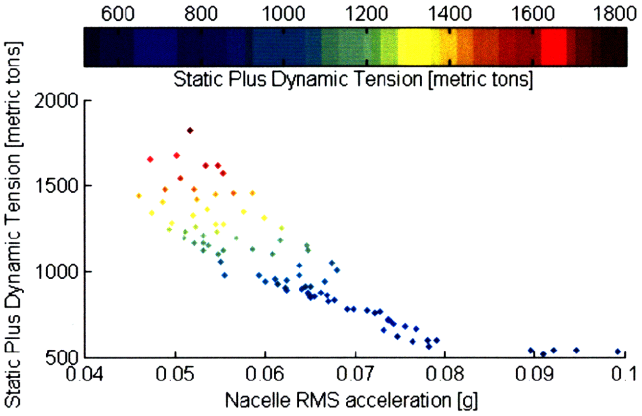

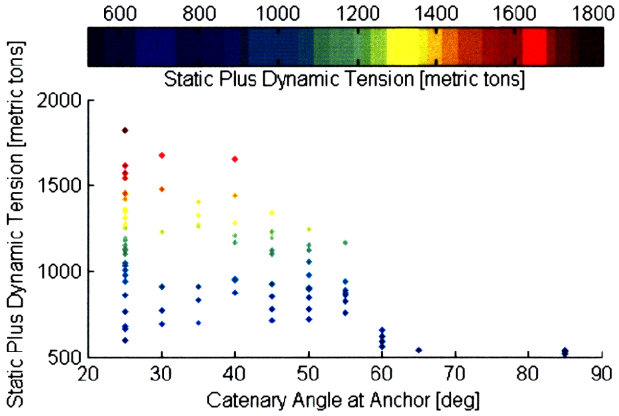

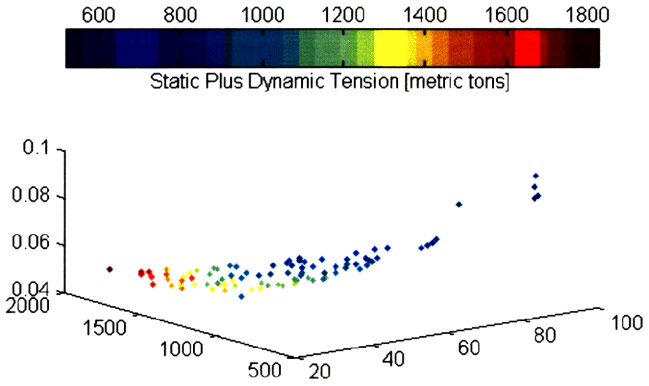

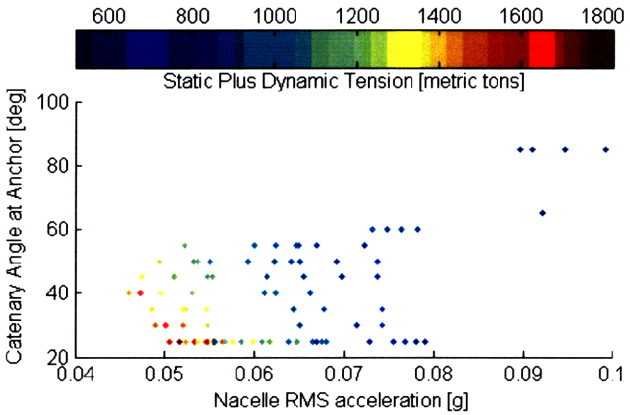

6. Conclusions

Based on the Pareto optimization analysis of floating wind turbines with SLC mooring system at water depth of 150 meter, the minimum static and dynamic tension acting on the anchor can be as low as 700 metric tons at ten meter sea state, and 500 metric tons at six meter sea state. In the designs with DLC mooring system, it can be as low as 600 metric tons at ten meter sea state, and 430 metric tons at six meter sea state. Regardless of the sea state and water depth, the RMS acceleration at nacelle has been shown to be mostly smaller than 0.12 g.

For the floating wind turbines at water depth of 300 meter, the static and dynamic tension appears to be relatively smaller than it is at water depth of 150 meter. This is the reason why more number of possible designs broadly exists along the alphas that it does at water depth of 150 meter. As the water depth becomes shallower, the dynamic performance becomes more challenging and harder to satisfy the design requirements than it is at deep water depths.

7. Future Work

The hydrodynamic characteristic of floating wind turbines obviously depends on the buoy dimension as well, which has been fixed at the present paper for the purpose of optimal mooring system designs. The optimal dimension of buoy needs to be determined by including the buoy dimension in design parameters.

The ballasted mooring line has not been taken accounted as one of the design parameters during the Pareto optimization analysis, and therefore it needs to be updated with additional input parameters; the mass and location of concrete ballast hanging down to a middle of each mooring line.

TLP is also one of the representative platforms in which most floating offshore structure are mounted, and therefore a detailed analysis and its comparison from the spar buoy structure needs to be performed in order to determine the optimal design for floating wind turbine systems.

Structural analysis also needs to be studied more thoroughly in order to accurately determine the optimal steel thickness for the platform.

8. References

1. Sclavounos, P. D., *Surface Waves and Their Interaction with Floating Bodies, Lecture Notes,* Massachusetts Institute of Technology, Cambridge, MA

2. N.F. Casey, Tuvnel, S.J. Banfield, TTI, "Factors Affecting Measurement of Axial Stiffness of Polyester Deepwater Mooring Rope Under Sinusoidal Loading", *Offshore Technology Conference,* May, 2005

3. Faltiensen, O.M. *Sea Loads on Ships and Offshore Structure, Cambridge,* UK: Cambridge University Press, 1999.

4. Tracy, C., *Parametric Design of Floating Wind Tubines,* Master of Science Thesis, Massachusetts Institute of Technology, 2007

5. Wayman, E.N., *Coupled Dynamics and Economic Analysis of Floating Wind Turbine Systems,* Master of Science Thesis, Massachusetts Institute of Technology, 2006

6. Jonkman, J.M., Sclavounos, P.D., "Development of Fully Coupled Aeroelastic and Hydrodynamic Models for Offshore Wind Turbines." *44th AIAA Aerospace Sciences Meeting and Exhibit*, January, 2006

7. Lee, K. H., *Responses of Floating Wind Turbines to Wind and Wave Excitation,* Master of Science Thesis, Massachusetts Institute of Technology, 2004

8. Lee, K. H., Sclavounos, P. D., Wayman, E. N., "Floating Wind Turbines," Workshop on Water Waves and Floating Bodies, May 29, 2005

9. Newman, J. N., *Marine Hydrodynamics,* Cambridge, MA: The MIT Press, 1977

10. Wayman, E.N., Sclavounos P.D., Butterfield S., Jonkman J., Musial W., "Coupled Dynamic Modeling of Floating Wind Turbine Systems," *Offshore Technology Conference,* May, 2006

11. C.H. Lee, *WAMIT THEORY* (Page 1~38) , *Research Project Report to Chevron, Conoco, Exxon, Mobil, Offshore Technology Research Center*, Dept of Ocean Engineering, Massachusetts Institute of Technology, 1995

12. WAMIT® (Chapter 1~7), *version 5.4*, Massachusetts Institute of Technology, 1998